Superradiance-like electron transport through a quantum dot

M. J. A. Schuetz,[1] E. M. Kessler,[1] J. I. Cirac,[1] and G. Giedke[1,2]
[1]*Max-Planck-Institut für Quantenoptik, Hans-Kopfermann-Strasse 1, 85748 Garching, Germany*
[2]*M5, Fakultät für Mathematik, TU München, L.-Boltzmannstrasse 1, 85748 Garching, Germany*
(Received 14 June 2012; published 27 August 2012)

We theoretically show that intriguing features of coherent many-body physics can be observed in electron transport through a quantum dot (QD). We first derive a master-equation-based framework for electron transport in the Coulomb-blockade regime which includes hyperfine (HF) interaction with the nuclear spin ensemble in the QD. This general tool is then used to study the leakage current through a single QD in a transport setting. We find that, for an initially polarized nuclear system, the proposed setup leads to a strong current peak, in close analogy with superradiant emission of photons from atomic ensembles. This effect could be observed with realistic experimental parameters and would provide clear evidence of coherent HF dynamics of nuclear spin ensembles in QDs.

DOI: 10.1103/PhysRevB.86.085322 PACS number(s): 85.35.Be, 76.70.Fz, 73.63.Kv, 42.50.Nn

I. INTRODUCTION

Quantum coherence is at the very heart of many intriguing phenomena in today's nanostructures.[1,2] For example, it is the essential ingredient to the understanding of the famous Aharonov-Bohm-like interference oscillations of the conductance of metallic rings[3] or the well-known conductance steps in quasi-one-dimensional wires.[4,5] In particular, nonequilibrium electronic transport has emerged as a versatile tool to gain deep insights into the coherent quantum properties of mesoscopic solid-state devices.[6,7] Here, with the prospect of spintronics and applications in quantum computing, a great deal of research has been directed towards the interplay and feedback mechanisms between electron and nuclear spins in gate-based semiconductor quantum dots.[8–14] Current fluctuations have been assigned to the random dynamics of the ambient nuclear spins[15] and/or hysteresis effects due to dynamic nuclear polarization.[15–18] Spin-flip-mediated transport, realized in few-electron quantum dots in the so-called spin-blockade regime,[19] has been shown to exhibit long time scale oscillations and bistability as a result of a buildup and relaxation of nuclear polarization.[15,16] The nuclear spins are known to act collectively on the electron spin via hyperfine interaction. In principle, this opens up an exciting test bed for the observation of collective effects which play a remarkable role in a wide range of many-body physics.[20–22]

In quantum optics, the concept of superradiance (SR), describing the cooperative emission of photons, is a paradigm example for a cooperative quantum effect.[1,23,24] Here, initially excited atoms emit photons collectively as a result of the buildup and reinforcement of strong interatomic correlations. Its most prominent feature is an emission intensity burst in which the system radiates much faster than an otherwise identical system of independent emitters. This phenomenon is of fundamental importance in quantum optics and has been studied extensively since its first prediction by Dicke in 1954.[23] Yet, in its original form the observation of optical SR has turned out to be difficult due to dephasing dipole-dipole van der Waals interactions, which suppress a coherence buildup in atomic ensembles.

This paper is built on analogies between mesoscopic solid-state physics and quantum optics: The nuclear spins surrounding a quantum dot (QD) are identified with an atomic ensemble, individual nuclear spins corresponding to the internal levels of a single atom and the electrons are associated with photons. Despite some fundamental differences—for example, electrons are fermions, whereas photons are bosonic particles—this analogy stimulates conjectures about the potential occurrence of related phenomena in these two fields of physics. Led by this line of thought, we address the question of whether superradiant behavior might also be observed in a solid-state environment where the role of photons is played by electrons. To this end, we analyze a gate-based semiconductor QD in the Coulomb blockade regime, obtaining two main results, of both experimental and theoretical relevance. First, in analogy to superradiant emission of photons, we show how to observe superradiant emission of electrons in a transport setting through a QD. We demonstrate that the proposed setup, when tuned into the spin-blockade regime, carries clear fingerprints of cooperative emission, with no van der Waals dephasing mechanism on relevant time scales. The spin blockade is lifted by the hyperfine (HF) coupling which becomes increasingly more efficient as correlations among the nuclear spins build up. This markedly enhances the spin-flip rate and hence the leakage current running through the QD. Second, we develop a general theoretical master-equation framework that describes the nuclear spin mediated transport through a single QD. Apart from the collective effects due to the HF interaction, the electronic tunneling current is shown to depend on the internal state of the ambient nuclear spins through the effective magnetic field (Overhauser field) produced by the hyperfine interaction.

The paper is structured as follows. In Sec. II, we highlight our key findings and provide an intuitive picture of our basic ideas, allowing the reader to grasp our main results on a qualitative level. By defining the underlying Hamiltonian, Sec. III then describes the system in a more rigorous fashion. Next, we present the first main result of this paper in Sec. IV: a general master equation for electron transport through a single QD which is coherently enhanced by the HF interaction with the ambient nuclear spins in the QD. It features both collective effects and feedback mechanisms between the electronic and the nuclear subsystem of the QD. Based on this theoretical

framework, Sec. V puts forward the second main result, namely the observation of superradiant behavior in the leakage current through a QD. The qualitative explanations provided in Sec. II should make it possible to read this part independently of the derivation given in Sec. IV. Section VI backs up our analytical predictions with numerical simulations. When starting from an initially polarized nuclear spin ensemble, the leakage current through the QD is shown to exhibit a strong peak whose relative height scales linearly with the number of nuclear spins, which we identify as the characteristic feature of superradiant behavior. In Sec. VII we draw conclusions and give an outlook on future directions of research.

II. MAIN RESULTS

In this section we provide an intuitive exposition of our key ideas and summarize our main findings.

HF-assisted electron transport. We study a single electrically defined QD in the Coulomb-blockade regime which is attached to two leads, as schematically depicted in Fig. 1. Formally, the Hamiltonian for the total system is given by

$$H = H_Z + H_B + H_T + H_{\mathrm{HF}}. \tag{1}$$

Here, H_Z describes the electronic level structure inside the QD in the presence of an external magnetic field. Next, H_B refers to two independent reservoirs of noninteracting electrons, the left and right leads, respectively. The coupling between these and the QD is described in terms of a tunneling Hamiltonian H_T and H_{HF} models the *collective* hyperfine interaction between an electron confined inside the QD and an ensemble of N proximal nuclear spins surrounding the QD. Note that the specific form of H is given later in Sec. III.

Our analysis is built on a quantum master-equation approach, a technique originally rooted in the field of quantum optics. By tracing out the unobserved degrees of freedom of the leads we derive an effective equation of motion for the density matrix of the QD system ρ_S—describing the electron spin inside the QD as well as the nuclear spin ensemble—irreversibly coupled to source and drain electron reservoirs. In addition to the standard assumptions of a weak system-reservoir coupling (Born approximation), a flat reservoir spectral density, and a short reservoir correlation time (Markov approximation), we demand the hyperfine flip-flops to be strongly detuned with respect to the effective magnetic field seen by the electron throughout the dynamics. Under these conditions, the central master equation can be written as

$$\begin{aligned}\dot{\rho}_S(t) = &-i[H_Z + H_{\mathrm{HF}}, \rho_S(t)] \\ &+ \sum_{\sigma=\uparrow,\downarrow} \alpha_\sigma(t)\left[d_\sigma \rho_S(t) d_\sigma^\dagger - \frac{1}{2}\{d_\sigma^\dagger d_\sigma, \rho_S(t)\}\right] \\ &+ \sum_{\sigma=\uparrow,\downarrow} \beta_\sigma(t)\left[d_\sigma^\dagger \rho_S(t) d_\sigma - \frac{1}{2}\{d_\sigma d_\sigma^\dagger, \rho_S(t)\}\right],\end{aligned} \tag{2}$$

where the tunneling rates $\alpha_\sigma(t)$ and $\beta_\sigma(t)$ describe dissipative processes by which an electron of spin σ tunnels from one of the leads into or out of the QD, respectively. Here, the fermionic operator $d_\sigma^\dagger$ creates an electron of spin σ inside the QD. While a detailed derivation of Eq. (2) along with the precise form of the tunneling rates is presented in Sec. IV, here we focus on a qualitative discussion of its theoretical and experimental implications. Essentially, our central master equation exhibits two core features.

Nuclear-state-dependent electronic dissipation. First, dissipation only acts on the electronic subsystem with rates $\alpha_\sigma(t)$ and $\beta_\sigma(t)$ that depend dynamically on the state of the nuclear subsystem. This nonlinear behavior potentially results in hysteretic behavior and feedback mechanisms between the two subsystems as already suggested theoretically[11,14,20,21] and observed in experiments in the context of double QDs in the Pauli-blockade regime (see, e.g., Refs. 12, 13, and 18). On a qualitative level, this finding can be understood as follows: The nuclear spins provide an effective magnetic field for the electron spin, the Overhauser field, whose strength is proportional to the polarization of the nuclear spin ensemble. Thus, a changing nuclear polarization can either dynamically tune or detune the position of the electron levels inside the QD. This, in turn, can have a marked effect on the transport properties of the QD as they crucially depend on the position of these resonances with respect to the chemical potentials of the leads. In our model, this effect is directly captured by the tunneling rates dynamically depending on the state of the nuclei.

SR in electron transport. Second, the collective nature of the HF interaction H_{HF} allows for the observation of coherent many-body effects. To show this, we refer to the following example: Consider a setting in which the bias voltage and an external magnetic field are tuned such that only one of the two electronic spin components, say the level $|\uparrow\rangle$, lies inside the transport window. In this spin-blockade regime the electrons tunneling into the right lead are spin-polarized; that is, the QD acts as a spin filter.[25,26] If the HF coupling is sufficiently small compared to the external Zeeman splitting, the electron

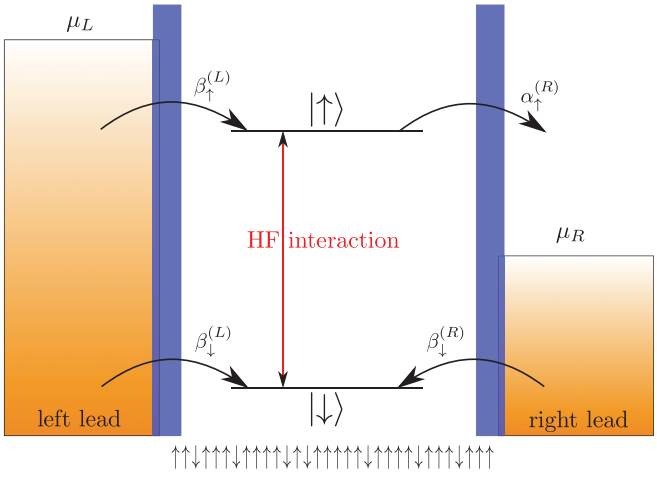

FIG. 1. (Color online) Schematic illustration of the transport system: An electrically defined QD is tunnel-coupled to two electron reservoirs, the left and right lead, respectively. A bias voltage $V = (\mu_L - \mu_R)/e$ is applied between the two leads in order to induce a current through the QD. An external magnetic field is used to tune the system into the sequential-tunneling regime and the QD effectively acts as a spin filter. The resulting spin blockade can be lifted by the HF interaction between the QD electron and the nuclear spins in the surrounding host environment.

is predominantly in its $|\downarrow\rangle$ spin state, making it possible to adiabatically eliminate the electronic QD coordinates. In this way we obtain an effective equation of motion for the nuclear density operator μ only. It reads

$$\dot{\mu} = c_r\left[A^-\mu A^+ - \frac{1}{2}\{A^+A^-,\mu\}\right] + ic_i[A^+A^-,\mu] + i\frac{g}{2}[A^z,\mu], \quad (3)$$

where $A^\mu = \sum_{i=1}^N g_i\sigma_i^\mu$ with $\mu = +,-,z$ are *collective* nuclear spin operators, composed of *all* N individual nuclear spin operators σ_i^μ, with g_i being proportional to the probability of the electron being at the location of the nucleus of site i. Again, we highlight the core implications of Eq. (3) and for a full derivation thereof, including the definition of the effective rates c_r and c_i, we refer to Sec. V. Most notably, Eq. (3) closely resembles the SR master equation which has been discussed extensively in the context of atomic physics[24] and therefore similar effects might be expected.

Superradiance is known as a macroscopic collective phenomenon which generalizes spontaneous emission from a single emitter to a many-body system of N atoms.[1] Starting from a fully polarized initial state the system evolves within a totally symmetric subspace under permutation and experiences a strong correlation buildup. As a consequence, the emission intensity is not of the usual exponentially decaying form, but conversely features a sudden peak occurring on a very rapid time scale $\sim 1/N$ with a maximum $\sim N^2$.

In this paper, we show that the same type of cooperative emission can occur from an ensemble of nuclear spins surrounding an electrically defined QD: The spin blockade can be lifted by the HF interaction as the nuclei pump excitations into the electron. Starting from a highly polarized, weakly correlated nuclear state (which could be prepared by, e.g., dynamic polarization techniques[12,13,22]), this process becomes increasingly more efficient, as correlations among the nuclei build up due to the collective nature of the HF interaction. This results in an increased leakage current. Therefore, the current is collectively enhanced by the electron's HF interaction with the ambient nuclear spin ensemble, giving rise to a superradiant-like effect in which the leakage current through the QD takes the role of the radiation field: To stress this relation, we also refer to this effect as *superradiant transport of electrons*.

Comparison to conventional SR. Compared to its conventional atomic counterpart, our system incorporates two major differences: First, our setup describes superradiant behavior from a *single* emitter, since in the strong Coulomb-blockade regime the electrons are emitted antibunched. As described above, the superradiant character is due to the nuclear spins acting collectively on the electron spin leading to an increased leakage current on time scales longer than single electron tunneling events. The second crucial difference is the *inhomogeneous* nature ($g_i \neq$ const) of the collective operators A^μ. Accordingly, the collective spin is not conserved, leading to dephasing between the nuclei which in principle could prevent the observation of superradiant behavior. However, as exemplified in Fig. 2, we show that under realistic conditions—taking into account a finite initial polarization of nuclear spins p and dephasing processes due to the inhomogeneous nature of the HF coupling—the leakage current through the QD still exhibits the characteristic peak whose relative height scales linearly with the number of nuclear spins. Even though the effect is reduced compared to the ideal case, for an experimentally realistic number of nuclei $N \approx 10^5$–10^6 a strong increase is still predicted. The experimental key signature of this effect, the relative peak height of the leakage current, can be varied by either tuning the external Zeeman splitting or the initial polarization of the nuclear spins.

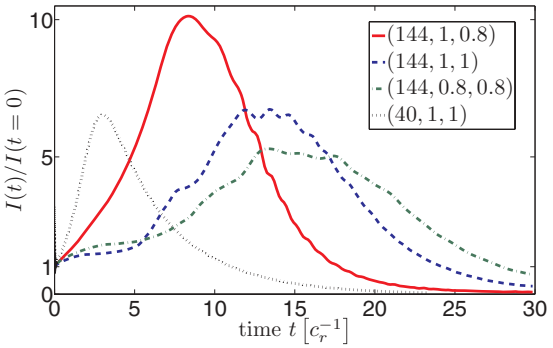

FIG. 2. (Color online) Normalized leakage current through a QD in the spin-blockade regime for N nuclear spins, initial nuclear polarization p, and external Zeeman splitting ω_0 in units of the total HF coupling constant $A_{\mathrm{HF}} \approx 100\ \mu$eV, summarized as $(N, p, \omega_0/A_{\mathrm{HF}})$. For homogeneous HF coupling the dynamics can be solved exactly (black dotted line). Compared to this idealized benchmark, the effects are reduced for realistic inhomogeneous HF coupling, but still present: The relative peak height becomes more pronounced for smaller detuning ω_0 or higher polarization p (solid red line compared to the blue dashed and green dash-dotted line, respectively). Even under realistic conditions, the relative peak height is found to scale linearly with N, corresponding to a strong enhancement for typically $N \approx 10^5$–10^6.

In the remainder of the paper, Eqs. (2) and (3) are derived from first principles; in particular, the underlying assumptions and approximations are listed. Based on this general theoretical framework, more results along with detailed discussions are presented. For both the idealized case of homogeneous HF coupling—in which an exact solution is feasible even for relatively large N—and the more realistic inhomogeneous case, further numerical simulations prove the existence of a strong superradiant peaking in the leakage current of single QD in the spin-blockade regime.

III. THE SYSTEM

This section gives an in-depth description of the Hamiltonian under study, formally introduced in Eq. (1). The system we consider consists of a single electrically defined QD in a transport setting as schematically depicted in Fig. 1. Due to strong confinement only a single orbital level is relevant. Moreover, the QD is assumed to be in the strong Coulomb-blockade regime so that at maximum one electron resides inside the QD. Therefore, the effective Hilbert space of the QD electron is span $\{|\uparrow\rangle, |\downarrow\rangle, |0\rangle\}$ where the lowest energy states for an additional electron in the QD with spin $\sigma = \uparrow, \downarrow$

are split by an external magnetic field. The Hamiltonian for the total system is given in Eq. (1).

Here, the first term,

$$H_Z = \sum_\sigma \epsilon_\sigma d_\sigma^\dagger d_\sigma, \tag{4}$$

describes the electronic levels of the QD. The Zeeman splitting between the two spin components is $\omega_0 = \epsilon_\uparrow - \epsilon_\downarrow$ (we set $\hbar = 1$) and the QD electron operators are $d_\sigma^\dagger = |\sigma\rangle\langle 0|$, describing transitions from the state $|0\rangle$ with no electron inside the QD to a state $|\sigma\rangle$ with one electron of spin σ inside the QD.

Electron transport through the QD is induced by attaching the QD to two electron leads (labeled as L and R), which are in thermal equilibrium at chemical potentials μ_L and μ_R, respectively. The leads themselves constitute reservoirs of noninteracting electrons,

$$H_B = \sum_{\alpha,k,\sigma} \epsilon_{\alpha k} c_{\alpha k\sigma}^\dagger c_{\alpha k\sigma}, \tag{5}$$

where $c_{\alpha k\sigma}^\dagger (c_{\alpha k\sigma})$ creates (annihilates) an electron in lead $\alpha = L, R$ with wave vector k and spin σ. The operators $c_{\alpha k\sigma}^\dagger (c_{\alpha k\sigma})$ fulfill the usual Fermi commutation relations: $\{c_{\alpha k\sigma}^\dagger, c_{\alpha' k'\sigma'}^\dagger\} = \{c_{\alpha k\sigma}, c_{\alpha' k'\sigma'}\} = 0$ and $\{c_{\alpha k\sigma}^\dagger, c_{\alpha' k'\sigma'}\} = \delta_{\alpha,\alpha'}\delta_{k,k'}\delta_{\sigma,\sigma'}$. The effect of the Coulomb interaction in the leads can be taken into account by renormalized effective quasiparticle masses. A positive source-drain voltage $V = (\mu_L - \mu_R)/e$ leads to a dominant tunneling of electrons from left to right. Microscopically, the coupling of the QD system to the electron reservoirs is described in terms of the tunneling Hamiltonian

$$H_T = \sum_{\alpha,k,\sigma} T_{k,\sigma}^{(\alpha)} d_\sigma^\dagger c_{\alpha k\sigma} + \text{H.c.}, \tag{6}$$

with the tunnel matrix element $T_{k,\sigma}^{(\alpha)}$ specifying the transfer coupling between the lead $\alpha = L, R$ and the system. There is no direct coupling between the leads and electron transfer is only possible by charging and discharging the QD.

The cooperative effects are based on the collective hyperfine interaction of the electronic spin of the QD with N initially polarized nuclear spins in the host environment of the QD.[27] It is dominated by the isotropic contact term[28] given by

$$H_{\text{HF}} = \frac{g}{2}(A^+ S^- + A^- S^+) + g A^z S^z. \tag{7}$$

Here S^μ and $A^\mu = \sum_{i=1}^N g_i \sigma_i^\mu$ with $\mu = +, -, z$ denote electron and collective nuclear spin operators, respectively. The coupling coefficients are normalized such that $\sum_i g_i^2 = 1$ and individual nuclear spin operators σ_i^μ are assumed to be spin-$\frac{1}{2}$ for simplicity; g is related to the total HF coupling strength A_{HF} via $g = A_{\text{HF}}/\sum_i g_i$. We neglect the typically very small nuclear Zeeman and nuclear dipole-dipole terms.[28] For simplicity, we also restrict our analysis to one nuclear species only. These simplifications are addressed in more detail in Sec. VI.

The effect of the HF interaction with the nuclear spin ensemble is twofold: The first part of the above Hamiltonian $H_{\text{ff}} = \frac{g}{2}(A^+ S^- + A^- S^+)$ is a Jaynes-Cummings-type interaction which exchanges excitations between the QD electron and the nuclei. The second term $H_{\text{OH}} = g A^z S^z$ constitutes a quantum magnetic field, the Overhauser field, for the electron spin generated by the nuclei. If the Overhauser field is not negligible compared to the external Zeeman splitting, it can have a marked effect on the current by (de)tuning the hyperfine flip-flops.

IV. GENERALIZED QUANTUM MASTER EQUATION

Electron transport through a QD can be viewed as a tool to reveal the QD's nonequilibrium properties in terms of the current-voltage I/V characteristics. From a theoretical perspective, a great variety of methods such as the scattering matrix formalism[29] and nonequilibrium Green's functions[7,30] have been used to explore the I/V characteristics of quantum systems that are attached to two metal leads. Our analysis is built upon the master equation formalism, a tool widely used in quantum optics for studying the irreversible dynamics of quantum systems coupled to a macroscopic environment.

In what follows, we employ a projection operator based technique to derive an effective master equation for the QD system—comprising the QD electron spin as well as the nuclear spins—which experiences dissipation via the electron's coupling to the leads. This dissipation is shown to dynamically depend on the state of the nuclear system potentially resulting in feedback mechanisms between the two subsystems. We derive conditions which allow for a Markovian treatment of the problem and list the assumptions our master equation based framework is based on.

A. Superoperator formalism: Nakajima-Zwanzig equation

The state of the global system that comprises the QD as well as the environment is represented by the full density matrix $\rho(t)$. However, the actual states of interest are the states of the QD which are described by the reduced density matrix $\rho_S = \mathsf{Tr}_\mathsf{B}[\rho]$, where $\mathsf{Tr}_\mathsf{B}\ldots$ averages over the unobserved degrees of freedom of the Fermi leads. We derive a master equation that governs the dynamics of the reduced density matrix ρ_S using the superoperator formalism. We start out from the von Neumann equation for the full density matrix

$$\dot\rho = -i[H(t), \rho], \tag{8}$$

where $H(t)$ can be decomposed into the following form which turns out to be convenient later on:

$$H(t) = H_0(t) + H_1(t) + H_T. \tag{9}$$

Here, $H_0(t) = H_Z + H_B + g\langle A^z\rangle_t S^z$ comprises the Zeeman splitting caused by the external magnetic field via H_Z and the Hamiltonian of the noninteracting electrons in the leads H_B; moreover, the time-dependent expectation value of the Overhauser field has been absorbed into the definition of $H_0(t)$. The HF interaction between the QD electron and the ensemble of nuclear spins has been split up into the flip-flop term H_{ff} and the Overhauser field H_{OH}, that is $H_{\text{HF}} = H_{\text{OH}} + H_{\text{ff}}$. The term $H_1(t) = H_{\Delta\text{OH}}(t) + H_{\text{ff}}$ comprises the Jaynes-Cummings-type dynamics H_{ff} and fluctuations due to deviations of the Overhauser field from its expectation value, that is, $H_{\Delta\text{OH}}(t) = g\delta A^z S^z$, where $\delta A^z = A^z - \langle A^z\rangle_t$.

The introduction of superoperators—operators acting on the space of linear operators on the Hilbert space—allows for a compact notation. The von Neumann equation is written

as $\dot{\rho} = -i\mathcal{L}(t)\rho$, where $\mathcal{L}(t) = \mathcal{L}_0(t) + \mathcal{L}_1(t) + \mathcal{L}_T$ is the Liouville superoperator defined via $\mathcal{L}_\alpha \cdot = [H_\alpha, \cdot]$. Next, we define the superoperator $\mathcal{P}$ as a projector onto the relevant subspace

$$\mathcal{P}\rho(t) = \mathsf{Tr}_B[\rho(t)] \otimes \rho_B^0 = \rho_S(t) \otimes \rho_B^0, \tag{10}$$

where ρ_B^0 describes separate thermal equilibria of the two leads whose chemical potentials are different due to the bias voltage $V = (\mu_L - \mu_R)/e$. Essentially, $\mathcal{P}$ maps a density operator onto one of product form with the environment in equilibrium but still retains the relevant information on the system state. The complement of $\mathcal{P}$ is $\mathcal{Q} = 1 - \mathcal{P}$.

By inserting $\mathcal{P}$ and $\mathcal{Q}$ in front of both sides of the von Neumann equation one can derive a closed equation for the projection $\mathcal{P}\rho(t)$, which for factorized initial condition, where $\mathcal{Q}\rho(0) = 0$, can be rewritten in the form of the generalized Nakajima-Zwanzig master equation,

$$\frac{d}{dt}\mathcal{P}\rho = -i\mathcal{P}\mathcal{L}\mathcal{P}\rho - \int_0^t dt'\, \mathcal{P}\mathcal{L}\mathcal{Q}\,\hat{T} e^{-i\int_{t'}^t d\tau \mathcal{Q}\mathcal{L}(\tau)} \mathcal{Q}\mathcal{L}\mathcal{P}\rho(t'), \tag{11}$$

which is nonlocal in time and contains all orders of the system-leads coupling.[31] Here, $\hat{T}$ denotes the chronological time-ordering operator. Since $\mathcal{P}$ and $\mathcal{Q}$ are projectors onto orthogonal subspaces that are only connected by $\mathcal{L}_T$, this simplifies to

$$\frac{d}{dt}\mathcal{P}\rho = -i\mathcal{P}\mathcal{L}\mathcal{P}\rho - \int_0^t dt' \mathcal{P}\mathcal{L}_T \hat{T} e^{-i\int_{t'}^t d\tau \mathcal{Q}\mathcal{L}(\tau)} \mathcal{L}_T \mathcal{P}\rho(t'). \tag{12}$$

Starting out from this exact integro-differential equation, we introduce some approximations: In the weak coupling limit we neglect all powers of $\mathcal{L}_T$ higher than two (Born approximation). Consequently, we replace $\mathcal{L}(\tau)$ with $\mathcal{L}(\tau) - \mathcal{L}_T$ in the exponential of Eq. (12). Moreover, we make use of the fact that the nuclear spins evolve on a time scale that is very slow compared to all electronic processes: In other words, the Overhauser field is quasistatic on the time scale of single electronic tunneling events.[22,32] That is, we replace $\langle A^z\rangle_\tau$ with $\langle A^z\rangle_t$ in the exponential of Eq. (12), which removes the explicit time dependence in the kernel. By taking the trace over the reservoir and using $\mathsf{Tr}_B[\mathcal{P}\dot{\rho}(t)] = \dot{\rho}_S(t)$, we get

$$\dot{\rho}_S(t) = -i(\mathcal{L}_Z + \mathcal{L}_{\rm HF})\rho_S(t) - \int_0^t d\tau\, \mathsf{Tr}_B(\mathcal{L}_T e^{-i[\mathcal{L}_0(t)+\mathcal{L}_1(t)]\tau} \times \mathcal{L}_T \mathcal{P}\rho(t-\tau)). \tag{13}$$

Here, we also used the relations $\mathcal{P}\mathcal{L}_T\mathcal{P} = 0$ and $\mathcal{L}_B\mathcal{P} = 0$ and switched the integration variable to $\tau = t - t'$. Note that, for notational convenience, we suppress the explicit time dependence of $\mathcal{L}_{0(1)}(t)$ in the following. In the next step, we iterate the Schwinger-Dyson identity:

$$e^{-i(\mathcal{L}_0+\mathcal{L}_1)\tau} = e^{-i\mathcal{L}_0\tau} - i\int_0^\tau d\tau'\, e^{-i\mathcal{L}_0(\tau-\tau')}\mathcal{L}_1 e^{-i(\mathcal{L}_0+\mathcal{L}_1)\tau'}. \tag{14}$$

In what follows, we keep only the first term of this infinite series (note that the next two leading terms are explicitly calculated in Appendix A). In quantum optics, this simplification is well known as an approximation of independent rates of variation.[33] In our setting it is valid, if $\mathcal{L}_1(t)$ is small compared to $\mathcal{L}_0(t)$ and if the bath correlation time τ_c is short compared to the HF dynamics, $A_{\rm HF} \ll 1/\tau_c$. Pictorially, this means that during the correlation time τ_c of a tunneling event, there is not sufficient time for the Rabi oscillation with frequency $g \lesssim A_{\rm HF}$ to occur. For typical materials,[34] the relaxation time τ_c is in the range of $\sim 10^{-15}$ s corresponding to a relaxation rate $\Gamma_c = \tau_c^{-1} \approx 10^5\,\mu$eV. Indeed, this is much faster than all other relevant processes. In this limit, the equation of motion for the reduced density matrix of the system simplifies to

$$\dot{\rho}_S(t) = -i(\mathcal{L}_Z + \mathcal{L}_{\rm HF})\rho_S(t) - \int_0^t d\tau\, \mathsf{Tr}_B\big(\mathcal{L}_T e^{-i\mathcal{L}_0(t)\tau}\mathcal{L}_T \rho_S(t-\tau)\otimes\rho_B^0\big). \tag{15}$$

Note, however, that this master equation is not Markovian as the rate of change of $\rho_S(t)$ still depends on its past. Conditions which allow for a Markovian treatment of the problem are addressed in the following.

B. Markov approximation

Using the general relation $e^{-i\mathcal{L}_0\tau}\mathcal{O} = e^{-iH_0\tau}\mathcal{O}e^{iH_0\tau}$ for any operator $\mathcal{O}$, we rewrite Eq. (15) as

$$\dot{\rho}_S(t) = -i[H_Z + H_{\rm HF}, \rho_S(t)] - \int_0^t d\tau\, \mathsf{Tr}_B\big([H_T, [\tilde{H}_T(\tau), e^{-iH_0\tau}\rho_S(t-\tau)e^{iH_0\tau}\otimes\rho_B^0]]\big). \tag{16}$$

In accordance with the previous approximations, we replace $e^{-iH_0\tau}\rho_S(t-\tau)e^{iH_0\tau}$ by $\rho_S(t)$ which is approximately the same since any correction to H_0 would be of higher order in perturbation theory.[35,36] In other words, the evolution of $\rho_S(t-\tau)$ is approximated by its unperturbed evolution, which is legitimate provided that the relevant time scale for this evolution τ_c is very short (Markov approximation). This step is motivated by the typically rapid decay of the lead correlations functions;[35] the precise validity of this approximation is elaborated below. In particular, this simplification disregards dissipative effects induced by H_T, which is valid self-consistently provided that the tunneling rates are small compared to the dynamics generated by H_0.

Moreover, in Eq. (16) we introduced the tunneling Hamiltonian in the interaction picture as $\tilde{H}_T(\tau) = e^{-iH_0\tau}H_T e^{iH_0\tau}$. For simplicity, we only consider one lead for now and add the terms referring to the second lead later on. Therefore, we can disregard an additional index specifying the left or right reservoir and write explicitly

$$\tilde{H}_T(\tau) = \sum_{k,\sigma} T_{k,\sigma} e^{-i[\epsilon_\sigma(t)-\epsilon_k]\tau} d_\sigma^\dagger c_{k\sigma} + \text{H.c.} \tag{17}$$

Here, the resonances $\epsilon_\sigma(t)$ are explicitly time dependent as they dynamically depend on the polarization of the nuclear spins

$$\epsilon_{\uparrow(\downarrow)}(t) = \epsilon_{\uparrow(\downarrow)} \pm \frac{g}{2}\langle A^z\rangle_t. \tag{18}$$

The quantity

$$\omega = \epsilon_\uparrow(t) - \epsilon_\downarrow(t) = \omega_0 + g\langle A^z\rangle_t \tag{19}$$

can be interpreted as an effective Zeeman splitting which incorporates the external magnetic field as well as the mean magnetic field generated by the nuclei.

Since the leads are assumed to be at equilibrium, their correlation functions are given by

$$\mathrm{Tr}_B\left[c^\dagger_{k\sigma}(\tau)c_{k'\sigma'}\rho_B^0\right] = \delta_{\sigma,\sigma'}\delta_{k,k'}e^{-i\epsilon_k\tau}f_k, \tag{20}$$

$$\mathrm{Tr}_B\left[c_{k\sigma}(\tau)c^\dagger_{k'\sigma'}\rho_B^0\right] = \delta_{\sigma,\sigma'}\delta_{k,k'}e^{i\epsilon_k\tau}(1-f_k), \tag{21}$$

where the Fermi function $f_k = (1+\exp[\beta(\epsilon_k-\mu)])^{-1}$ with inverse temperature $\beta = 1/(k_BT)$ gives the thermal occupation number of the respective lead in equilibrium. Note that all terms comprising two lead creation $c^\dagger_{k\sigma}$ or annihilation operators $c_{k\sigma}$ vanish since ρ_B^0 contains states with definite electron number only.[35] The correlation functions are diagonal in spin space and the tunneling Hamiltonian preserves the spin projection; therefore, only corotating terms prevail. If we evaluate all dissipative terms appearing in Eq. (16), due to the conservation of momentum and spin in Eqs. (20) and (21), only a single sum over k,σ survives. Here, we single out one term explicitly, but all other terms follow analogously. We obtain

$$\dot\rho_S(t) = \cdots + \sum_\sigma \int_0^t d\tau\, \mathcal{C}_\sigma(\tau) d^\dagger_\sigma e^{-iH_0\tau}\rho_S(t-\tau)e^{iH_0\tau}d_\sigma, \tag{22}$$

where the correlation time of the bath τ_c is determined by the decay of the noise correlations,

$$\mathcal{C}_\sigma(\tau) = \sum_k |T_{k,\sigma}|^2 f_k e^{i[\epsilon_\sigma(t)-\epsilon_k]\tau} = \int_0^\infty d\epsilon\, J_\sigma(\epsilon)e^{i[\epsilon_\sigma(t)-\epsilon]\tau}. \tag{23}$$

Here, we made use of the fact that the leads are macroscopic and therefore exhibit a continuous density of states per spin $n(\epsilon)$. On top of that, we have introduced the spectral density of the bath as

$$J_\sigma(\epsilon) = D_\sigma(\epsilon)f(\epsilon), \tag{24}$$

where $D_\sigma(\epsilon) = n(\epsilon)|T_\sigma(\epsilon)|^2$ is the effective density of states. The Markovian treatment manifests itself in a self-consistency argument: We assume that the spectral density of the bath $J_\sigma(\epsilon)$ is flat around the (time-dependent) resonance $\epsilon_\sigma(t)$ over a range set by the characteristic width Γ_d. Typically, both the tunneling matrix elements $T_\sigma(\epsilon)$ as well as the density of states $n(\epsilon)$ are slowly varying functions of energy. In the so-called wide-band limit the effective density of states $D_\sigma(\epsilon)$ is assumed to be constant so that the self-consistency argument will exclusively concern the behavior of the Fermi function $f(\epsilon)$, which is intimately related to the temperature of the bath T. Under the condition, that $J_\sigma(\epsilon)$ behaves flat on the scale Γ_d, it can be replaced with its value at $\epsilon_\sigma(t)$, and the noise correlation simplifies to

$$\mathcal{C}_\sigma(\tau) = J_\sigma(\epsilon_\sigma(t))e^{i\epsilon_\sigma(t)\tau}\int_0^\infty d\epsilon\, e^{-i\epsilon\tau}. \tag{25}$$

Using the relation

$$\int_0^\infty d\epsilon\, e^{-i\epsilon\tau} = \pi\delta(\tau) - i\mathbb{P}\frac{1}{\tau}, \tag{26}$$

with $\mathbb{P}$ denoting Cauchy's principal value, we find that the Markov approximation $\mathrm{Re}[\mathcal{C}_\sigma(\tau)] \propto \delta(\tau)$ is fulfilled provided that the self-consistency argument holds. This corresponds to the white-noise limit where the correlation-time of the bath is $\tau_c = 0$. Pictorially, the reservoir has no memory and instantaneously relaxes to equilibrium. We can then indeed replace $e^{-iH_0\tau}\rho_S(t-\tau)e^{iH_0\tau}$ with $\rho_S(t)$ and extend the integration in Eq. (16) to infinity, with negligible contributions due to the rapid decay of the memory kernel. In the following, we derive an explicit condition for the self-consistency argument to be satisfied.

Let us first consider the limit $T = 0$: As schematically depicted in Fig. 3, in this case $f(\epsilon)$ behaves perfectly flat except for $\epsilon = \mu$, where the self-consistency argument is violated. Therefore, the Markovian approximation is valid at $T = 0$ given that the condition $|\epsilon_\sigma(t) - \mu| \gg \Gamma_\mathrm{d}$ is fulfilled. In this limit, all tunneling rates are constant over time and effectively decoupled from the nuclear dynamics. Note that for the observation of superradiant transport it is sufficient to restrict oneself to this case.

For a more general analysis, we now turn to the case of finite temperature $T > 0$. We require the absolute value of the relative change of the Fermi function around the resonance $\epsilon_\sigma(t)$ over a range of the characteristic width Γ_d to be much less than unity, that is,

$$\left|\frac{\partial f(\epsilon)}{\partial\epsilon}\Big|_{\epsilon_\sigma(t)}\right|\Gamma_\mathrm{d} \ll 1. \tag{27}$$

An upper bound for the first factor can easily be obtained as this quantity is maximized at the chemical potential μ, for all temperatures. Evaluating the derivative at $\epsilon_\sigma(t) = \mu$ results in the compact condition,

$$\Gamma_\mathrm{d} \ll 4k_BT. \tag{28}$$

Thus, finite temperature $T > 0$ washes out the rapid character of $f(\epsilon)$ at the chemical potential μ and, provided that Eq. (28) is fulfilled, allows for a Markovian treatment.

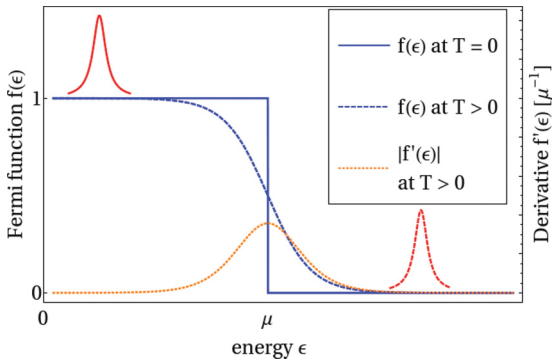

FIG. 3. (Color online) Fermi function for finite temperature (dashed blue line) and in the limit $T = 0$ (solid blue line). The absolute value of the derivative of the Fermi function $f'(\epsilon)$ (dotted orange line for finite temperature) is maximized at the chemical potential μ and tends to a δ function in the limit $T \to 0$. The Markovian description is valid provided that the Fermi function is approximately constant around the resonances $\epsilon_\sigma(t)$ on a scale of the width of these resonances, schematically shown in red [solid line for $\epsilon_\sigma(t) < \mu$ and dashed line for $\epsilon_\sigma(t) > \mu$].

Two distinct mechanisms contribute to the width Γ_d: dissipation due to coupling to the leads and the effect of $H_1(t)$. Both of them have been neglected self-consistently in the memory kernel when going from Eq. (12) to Eq. (15). Typically, the tunneling rates are of the order of ∼5–20 μeV, depending on the transparency of the tunnel barrier. Regarding the contribution due to $H_1(t)$, we first consider two limits of particular importance: For a completely mixed state the fluctuation of the nuclear field around its zero expectation value is of the order of $\sim A_{\rm HF}/\sqrt{N} \approx 0.1\,\mu$eV. In contrast, for a fully polarized state these fluctuations can be neglected, whereas the effective strength of the flip-flop dynamics is $\sim A_{\rm HF}/\sqrt{N}$ as well. Therefore, in both limits considered here, the dominant contribution to Γ_d is due to the coupling to the leads and the self-consistency condition could still be met with cryostatic temperatures $k_B T \gtrsim 10\,\mu$eV, well below the orbital level spacing. However, we note that in the course of a superradiant evolution, where strong correlations among the nuclei build up, the dominant contribution to Γ_d may come from the flip-flop dynamics, which are $A_{\rm HF}/4 \approx 25\,\mu$eV at maximum for homogeneous coupling. For realistic conditions, though, this effect is significantly reduced, as demonstrated in our simulations in Sec. VI.

C. General master equation for nuclear spin-assisted transport

Assuming that the self-consistency argument for a Markovian treatment is satisfied, we now apply the following modifications to Eq. (16): First, we neglect level shifts due to the coupling to the continuum states which can be incorporated by replacing the bare frequencies $\epsilon_\sigma(t)$ with renormalized frequencies. Second, one adds the second electron reservoir that has been omitted in the derivation above. Last, one performs a suitable transformation into a frame rotating at the frequency $\bar{\epsilon} = (\epsilon_\uparrow + \epsilon_\downarrow)/2$ leaving all terms invariant but changing H_Z from $H_Z = \epsilon_\uparrow d_\uparrow^\dagger d_\uparrow + \epsilon_\downarrow d_\downarrow^\dagger d_\downarrow$ to $H_Z = \omega_0 S^z$. After these manipulations one arrives at the central master equation as stated in Eq. (2) where the tunneling rates with $\alpha_\sigma(t) = \sum_{x=L,R} \alpha_\sigma^{(x)}(t)$, $\beta_\sigma(t) = \sum_{x=L,R} \beta_\sigma^{(x)}(t)$, and

$$\begin{aligned} \frac{\alpha_\sigma^{(x)}(t)}{2\pi} &= n_x(\epsilon_\sigma(t))\left|T_\sigma^{(x)}(\epsilon_\sigma(t))\right|^2[1 - f_x(\epsilon_\sigma(t))], \\ \frac{\beta_\sigma^{(x)}(t)}{2\pi} &= n_x(\epsilon_\sigma(t))\left|T_\sigma^{(x)}(\epsilon_\sigma(t))\right|^2 f_x(\epsilon_\sigma(t)) \end{aligned} \tag{29}$$

govern the dissipative processes in which the QD system exchanges single electrons with the leads. The tunneling rates, as presented here, are widely used in nanostructure quantum transport problems.[35,37,38] However, in our setting they are evaluated at the resonances $\epsilon_\sigma(t)$ which dynamically depend on the polarization of the nuclear spins [see Eq. (18)]. Note that Eq. (2) incorporates finite temperature effects via the Fermi functions of the leads. This potentially gives rise to feedback mechanisms between the electronic and the nuclear dynamics, since the purely electronic diffusion markedly depends on the nuclear dynamics.

Since Eq. (2) marks our first main result, at this point we quickly reiterate the assumptions our master equation treatment is based on.

(i) The system-lead coupling is assumed to be weak and therefore treated perturbatively up to second order (Born approximation).

(ii) In particular, the tunneling rates are small compared to the effective Zeeman splitting ω.

(iii) Level shifts arising from the coupling to the continuum states in the leads are merely incorporated into a redefinition of the QD energy levels $\epsilon_\sigma(t)$.

(iv) There is a separation of time scales between electron-spin dynamics and nuclear-spin dynamics. In particular, the Overhauser field $g\langle A^z\rangle_t$ evolves on a time scale that is slow compared to single electron tunneling events.

(v) The HF dynamics generated by $H_1(t) = H_{\rm ff} + H_{\Delta\rm OH}(t)$ is (i) sufficiently weak compared to H_0 and (ii) slow compared to the correlation time of the bath τ_c, which is $A_{\rm HF}\tau_c \ll 1$ (approximation of independent rates of variation). Note that the flip-flop dynamics can become very fast as correlations among the nuclei build up culminating in a maximum coupling strength of $A_{\rm HF}/4$ for homogeneous coupling. This potentially drives the system into the strong coupling regime where condition (i), that is $\omega \gg ||H_1(t)||$, might be violated. However, under realistic conditions of inhomogeneous coupling this effect is significantly reduced.

(vi) The effective density of states $D_\sigma(\epsilon) = n(\epsilon)|T_\sigma(\epsilon)|^2$ is weakly energy dependent (wide-band limit). In particular, it is flat on a scale of the characteristic widths of the resonances.

(vii) The Markovian description is valid provided that either the resonances are far away from the chemical potentials of the leads on a scale set by the characteristic widths of the resonances or the temperature is sufficiently high to smooth out the rapid character of the Fermi functions of the leads. This condition is quantified in Eq. (28).

In summary, we have derived a quantum master equation describing electronic transport through a single QD which is collectively enhanced due to the interaction with a large ancilla system, namely the nuclear spin ensemble in the host environment. Equation (2) incorporates two major intriguing features both of theoretical and experimental relevance: Due to a separation of time scales, only the electronic subsystem experiences dissipation with rates that depend dynamically on the state of the ancilla system. This nonlinearity gives rise to feedback mechanisms between the two subsystems as well as hysteretic behavior. Moreover, the collective nature of the HF interaction offers the possibility to observe intriguing coherent many-body effects. Here, one particular outcome is the occurrence of superradiant electron transport, as shown in the remainder of this paper.

Note that in the absence of HF interaction between the QD electron and the proximal nuclear spins, that is, in the limit $g \to 0$, our results agree with previous theoretical studies.[36]

V. SUPERRADIANCE-LIKE ELECTRON TRANSPORT

Proceeding from our general theory derived above, this section is devoted to the prediction and analysis of superradiant behavior of nuclear spins, evidenced by the strongly enhanced leakage current through a single QD in the Coulomb-blockade regime; see Fig. 1 for the scheme of the setup. A pronounced peak in the leakage current will serve as the main evidence for SR behavior in this setting.

We note that, in principle, an enhancement seen in the leakage current could also simply arise from the Overhauser field dynamically tuning the hyperfine flip-flops. However, we can still ensure that the measured change in the leakage current through the QD is due to cooperative emission only by dynamically compensating the Overhauser field. This can be achieved by applying a time-dependent magnetic or spin-dependent ac Stark field such that $H_{\rm comp}(t) = -g\langle A^z\rangle_t S^z$, which is done in most of our simulations below to clearly prove the existence of superradiant behavior in this setting. Consequently, in our previous analysis $H_0(t)$ is replaced with $H_0 = H_0(t) - g\langle A^z\rangle_t S^z = H_Z + H_B$ so that the polarization dependence of the tunneling rates is removed and we can drop the explicit time dependence of the resonances $\epsilon_\sigma(t) \to \epsilon_\sigma$. Under this condition, the master equation for the reduced system density operator can be written as

$$\begin{aligned}\dot\rho_S(t) = &-i[\omega_0 S^z + H_{\rm HF} + H_{\rm comp}(t), \rho_S(t)] \\ &+ \sum_{\sigma=\uparrow,\downarrow} \alpha_\sigma \left[d_\sigma \rho_S(t) d_\sigma^\dagger - \frac{1}{2}\{d_\sigma^\dagger d_\sigma, \rho_S(t)\}\right] \\ &+ \sum_{\sigma=\uparrow,\downarrow} \beta_\sigma \left[d_\sigma^\dagger \rho_S(t) d_\sigma - \frac{1}{2}\{d_\sigma d_\sigma^\dagger, \rho_S(t)\}\right]. \end{aligned} \tag{30}$$

In accordance with our previous considerations, in this specific setting the Markovian treatment is valid provided that the spectral density of the reservoirs varies smoothly around the (time-independent) resonances ϵ_σ on a scale set by the natural widths of the level and the fluctuations of the dynamically compensated Overhauser field. More specifically, throughout the whole evolution the levels are assumed to be far away from the chemical potentials of the reservoirs;[39,40] for an illustration see Fig. 3. In this wide-band limit, the tunneling rates $\alpha_\sigma, \beta_\sigma$ are independent of the state of the nuclear spins. The master equation is of Lindblad form which guarantees the complete positivity of the generated dynamics. Equation (30) agrees with previous theoretical results,[36] except for the appearance of the collective HF interaction between the QD electron and the ancilla system in the Hamiltonian dynamics of Eq. (30).

To some extent, Eq. (30) bears some similarity with the quantum theory of the laser. While in the latter the atoms interact with bosonic reservoirs, in our transport setting the QD is pumped by the nuclear spin ensemble and emits fermionic particles.[30,38]

If the HF dynamics is the slowest time scale in the problem, Eq. (30) can be recast into a form which makes its superradiant character more apparent. In this case, the system is subject to the slaving principle:[30] The dynamics of the whole system follow that of the subsystem with the slowest time constant, making it possible to adiabatically eliminate the electronic QD coordinates and to obtain an effective equation of motion for the nuclear spins. In this limit, the Overhauser field is much smaller than the Zeeman splitting so that a dynamic compensation of the OH can be disregarded for the moment. For simplicity, we consider a transport setting in which only four tunneling rates are different from zero (see Fig. 1). The QD can be recharged from the left and the right lead, but only electrons with spin projection $\sigma = \uparrow$ can tunnel out of the QD into the right lead. We define the total recharging rate $\beta = \beta_\downarrow + \beta_\uparrow = \beta_\downarrow^{(L)} + \beta_\downarrow^{(R)} + \beta_\uparrow^{(L)}$ and for notational convenience unambiguously set $\alpha = \alpha_\uparrow^{(R)}$. First, we project Eq. (30) onto the populations of the electronic levels and the coherences in spin space according to $\rho_{mn} = \langle m|\rho_S|n\rangle$, where $m,n = 0, \uparrow, \downarrow$. This yields

$$\dot\rho_{00} = \alpha\rho_{\uparrow\uparrow} - \beta\rho_{00}, \tag{31}$$

$$\begin{aligned}\dot\rho_{\uparrow\uparrow} = &-i\frac{g}{2}[A^z,\rho_{\uparrow\uparrow}] - i\frac{g}{2}(A^-\rho_{\downarrow\uparrow} - \rho_{\uparrow\downarrow}A^+) \\ &- \alpha\rho_{\uparrow\uparrow} + \beta_\uparrow\rho_{00},\end{aligned} \tag{32}$$

$$\dot\rho_{\downarrow\downarrow} = +i\frac{g}{2}[A^z,\rho_{\downarrow\downarrow}] - i\frac{g}{2}(A^+\rho_{\uparrow\downarrow} - \rho_{\downarrow\uparrow}A^-) + \beta_\downarrow\rho_{00}, \tag{33}$$

$$\begin{aligned}\dot\rho_{\uparrow\downarrow} = &-i\omega_0\rho_{\uparrow\downarrow} - i\frac{g}{2}(A^z\rho_{\uparrow\downarrow} + \rho_{\uparrow\downarrow}A^z) \\ &- i\frac{g}{2}(A^-\rho_{\downarrow\downarrow} - \rho_{\uparrow\uparrow}A^-) - \frac{\alpha}{2}\rho_{\uparrow\downarrow}.\end{aligned} \tag{34}$$

We can retrieve an effective master equation for the regime in which on relevant time scales the QD is always populated by an electron. This holds for a sufficiently strong recharging rate, that is in the limit $\beta \gg \alpha$, which can be implemented experimentally by making the left tunnel barrier more transparent than the right one. Then, the state $|0\rangle$ is populated negligibly throughout the dynamics and can be eliminated adiabatically according to $\rho_{00} \approx \frac{\alpha}{\beta}\rho_{\uparrow\uparrow}$. In analogy to the Anderson impurity model, in the following this limit is referred to as *local moment regime*. The resulting effective master equation reads

$$\begin{aligned}\dot\rho_S = &-i[\omega_0 S^z + H_{\rm HF}, \rho_S] + \gamma\left[S^-\rho_S S^+ - \frac{1}{2}\{S^+S^-,\rho_S\}\right] \\ &+ \Gamma\left[S^z\rho_S S^z - \frac{1}{4}\rho_S\right],\end{aligned} \tag{35}$$

where

$$\gamma = \frac{\beta_\downarrow}{\beta}\alpha \tag{36}$$

is an effective decay rate and

$$\Gamma = \frac{\beta_\uparrow}{\beta}\alpha \tag{37}$$

represents an effective electronic dephasing rate. This situation is schematized in Fig. 4. The effective decay (dephasing) describes processes in which the QD is recharged with a spin down (up) electron after a spin up electron has tunneled out of the QD. As demonstrated in Ref. 41, additional electronic dephasing mechanisms only lead to small corrections to the dephasing rate Γ and are therefore neglected in Eq. (35).

In the next step we aim for an effective description that contains only the nuclear spins: Starting from a fully polarized state, SR is due to the increase in the operative HF matrix element $\langle A^+A^-\rangle$. The scale of the coupling is set by the total HF coupling constant $A_{\rm HF} = g\sum_i g_i$. For a sufficiently small *relative coupling strength*[27]

$$\epsilon = A_{\rm HF}/(2\Delta), \tag{38}$$

where

$$\Delta = |\alpha/2 + i\omega_0|, \tag{39}$$

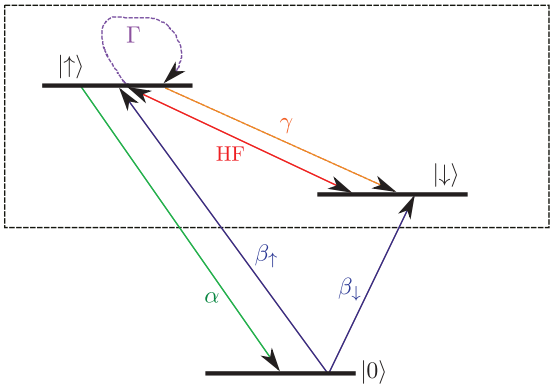

FIG. 4. (Color online) The electronic QD system in the local moment regime after the adiabatic elimination of the $|0\rangle$ level including the relevant dissipative processes. Within the effective system (box) we encounter an effective decay term and an effective pure dephasing term, with the rates γ and Γ, respectively. This simplification is possible for fast recharging of the QD, that is, $\beta \gg \alpha$.

the electron is predominantly in its $|\downarrow\rangle$ spin state and we can project Eq. (35) to the respective subspace. As shown in detail in Appendix B, in this limit the master equation for the reduced nuclear density operator $\mu = \mathrm{Tr}_{\mathrm{el}}[\rho_S]$ is given by Eq. (3), where the effective coefficients read

$$c_r = \frac{g^2\alpha}{4\Delta^2}, \tag{40}$$

$$c_i = \frac{g^2\omega_0}{4\Delta^2}. \tag{41}$$

This master equation is our second main result. In an optical setting, it has previously been predicted theoretically to exhibit strong SR signatures.[27] Conceptually, its superradiant character can be understood immediately in the ideal case of homogeneous coupling in which the collective state of all nuclear spins can be described in terms of Dicke states $|J,m\rangle$: The enhancement of the HF interaction is directly associated with the transition through nuclear Dicke states $|J,m\rangle, m \ll J$. In this idealized setting, the angular momentum operator $\mathbf{I} = \sqrt{N}\mathbf{A}$ of the nuclear spin ensemble obeys the SU(2) Lie algebra, from which one can deduce the ladder operator relation $I^-|J,m\rangle = \sqrt{J(J+1) - m(m-1)}|J,m-1\rangle$. This means that, starting from an initially fully polarized state $|J = N/2, m = N/2\rangle$, the nuclear system cascades down the Dicke ladder with an effective rate

$$\tilde{\Gamma}_{m\to m-1} = \frac{c_r}{N}(N/2+m)(N/2-m+1), \tag{42}$$

since, according to the first term in Eq. (3), the populations of the Dicke states evolve as

$$\dot{\mu}_{m,m} = -\frac{c_r}{N}(N/2+m)(N/2-m+1)\mu_{m,m} + \frac{c_r}{N}(N/2+m+1)(N/2-m)\mu_{m+1,m+1}. \tag{43}$$

While the effective rate is $\tilde{\Gamma}_{N/2\to N/2-1} = c_r$ at the very top of the the ladder it increases up to $\tilde{\Gamma}_{|m|\ll N/2} \approx \frac{c_r}{4}N$ at the center of the Dicke ladder. This implies the characteristic intensity peaking as compared to the limit of independent classical emitters the emission rate of which would be $\tilde{\Gamma}_{\mathrm{cl}} = \frac{c_r}{N}N_\uparrow = \frac{c_r}{N}(N/2+m)$.

However, there is also a major difference compared to the superradiant emission of photons from atomic ensembles: In contrast to its atomic cousin, the prefactor $c_r/N \propto 1/N^2$ is N-dependent, resulting in an overall time of the SR evolution $\langle t_D\rangle$ which increases with N. By linearizing Eq. (42) for the beginning of the superradiant evolution[24] as $\tilde{\Gamma}_{m\to m-1} \approx c_r(s+1)$, where $s = N/2 - m$ gives the number of nuclear flips, one finds that the first flip takes place in an average time c_r^{-1}, the second one in a time $(2c_r)^{-1}$, and so on. The summation of all these elementary time intervals gives an upper bound estimate for the process duration until the SR peaking as

$$\langle t_D\rangle \lesssim \frac{2}{c_r}\left[1 + \frac{1}{2} + \cdots + \frac{1}{N/2}\right] \approx \frac{2\ln(N/2)}{c_r}, \tag{44}$$

which, indeed, increases with the number of emitters as $\sim N\ln(N)$, whereas one obtains $\langle t_D\rangle \sim \ln(N)/N$ for ordinary SR.[24] Accordingly, in our solid-state system the characteristic SR peak appears at later times for higher N. The underlying reason for this difference is that in the atomic setting each new emitter adds to the overall coupling strength, whereas in the central spin setting a fixed overall coupling strength A_{HF} is distributed over an increasing number of particles. Note that in an actual experimental setting N is not a tunable parameter, of course. For our theoretical discussion, though, it is convenient to fix the total HF coupling strength A_{HF} and to extrapolate from our findings to an experimentally relevant number of nuclear spins N.

For large relative coupling strength $\epsilon \gg 1$ the QD electron saturates and superradiant emission is capped by the decay rate $\alpha/2$, prohibiting the observation of a strong intensity peak. In order to circumvent this bottleneck regime, one has to choose a detuning ω_0 such that $0 < \epsilon \leqslant 1$. However, to realize the spin-blockade regime, where the upper spin manifold is energetically well separated from the lower spin manifold, the Zeeman splitting has to be of the order of $\omega_0 \sim A_{\mathrm{HF}}$, which guarantees $\epsilon < 1$. In this parameter range, the early stage of the evolution—in which the correlation buildup necessary for SR takes place[24]—is well described by Eq. (3).

The inhomogeneous nature ($g_i \neq$ const) of the collective operators A^μ leads to dephasing between the nuclei, possibly preventing the phased emission necessary for the observation of SR.[24,27,42,43] The inhomogeneous part of the last term in Eq. (3)—the electron's Knight field—causes dephasing[44] $\propto g\sqrt{\mathrm{Var}(g_i)}/2$, possibly leading to symmetry reducing transitions $J \to J-1$. Still, it has been shown that SR is also present in realistic inhomogeneous systems,[27] since the system evolves in a many-body protected manifold (MPM): The second term in Eq. (3) energetically separates different total nuclear spin-J manifolds, protecting the correlation buildup for large enough ϵ.

The superradiant character of Eq. (3) suggests the observation of its prominent intensity peak in the leakage current through the QD in the spin-blockade regime. We have employed the method of full-counting-statistics (FCS)[45,46] in order to obtain an expression for the current and find (setting the electron's charge $e = 1$)

$$I(t) = \alpha\rho_{\uparrow\uparrow} - \beta_\downarrow^{(R)}\rho_{00}. \tag{45}$$

This result is in agreement with previous theoretical findings: The current through the device is completely determined by

the occupation of the levels adjacent to one of the leads.[29,37,39] The first term describes the accumulation of electrons with spin $\sigma = \uparrow$ in the right lead, whereas the second term describes electrons with $\sigma = \downarrow$ tunneling from the right lead into the QD. As done before,[27] we take the ratio of the maximum current to the initial current (the maximum for independent emitters) $I_{\mathrm{coop}}/I_{\mathrm{ind}}$ as our figure of merit: A relative intensity peak height $I_{\mathrm{coop}}/I_{\mathrm{ind}} > 1$ indicates cooperative effects. One of the characteristic features of SR is that this quantity scales linearly with the number of spins N.

In the local-moment regime, described by Eq. (35), the expression for the current simplifies to $I(t) = (1 - \beta_{\downarrow}^{(R)}/\beta)\alpha\langle S^+S^-\rangle_t \propto \langle S^+S^-\rangle_t$, showing that it is directly proportional to the electron inversion. This, in turn, increases as the nuclear system pumps excitations into the electronic system. A compact expression for the relation between the current and the dynamics of the nuclear system can be obtained immediately in the case of homogeneous coupling,

$$\frac{d}{dt}\langle S^+S^-\rangle_t = -\frac{d}{dt}\langle I^z\rangle_t - \gamma\langle S^+S^-\rangle_t. \tag{46}$$

Since the nuclear dynamics are, in general, much slower than the electron's dynamics, the approximate solution of this equation is $\langle S^+S^-\rangle_t \approx -\frac{d}{dt}\langle I^z\rangle_t/\gamma$. As a consequence, the current $I(t)$ is proportional to the time-derivative of the nuclear polarization,

$$I(t) \propto -\frac{d}{dt}\langle I^z\rangle_t. \tag{47}$$

Still, no matter how strong the cooperative effects are, on a time scale of single electron tunneling events, the electrons will always be emitted antibunched, since in the strong Coulomb-blockade regime the QD acts as a single-electron emitter.[47] Typically, the rate for single-electron emission events is even below the tunneling rate α due to the spin blockade. On electronic time scales $\sim 1/\alpha$, the SR mechanism manifests in lifting this blockade; as argued above, the efficiency of this process is significantly enhanced by collective effects.

Before we proceed with an in-depth analysis of the current $I(t)$, we note that an intriguing extension of the present work would be the study of fluctuations thereof (see, for example, Ref. 48 for studies of the shot noise spectrum in a related system). Insights into the statistics of the current could be obtained by analyzing two-time correlation functions such as $\langle n_\uparrow(t+\tau)n_\uparrow(t)\rangle$, where $n_\uparrow = d_\uparrow^\dagger d_\uparrow$. This can conveniently be done via the Quantum Regression Theorem,[49] which yields the formal result $\langle n_\uparrow(t+\tau)n_\uparrow(t)\rangle = \mathrm{Tr}_S[n_\uparrow e^{\mathcal{W}\tau}(n_\uparrow\rho_S(t))]$. Here, $\mathcal{W}$ denotes the Liouvillian governing the system's dynamics according to $\dot\rho_S = \mathcal{W}\rho_S$ [see Eq. (35)] and $\mathrm{Tr}_S[\cdots]$ refers to the trace over the system's degree of freedoms. This procedure can be generalized to higher-order correlation functions and full evaluation of the current statistics might reveal potential connections between current fluctuations and cooperative nuclear dynamics.

VI. ANALYSIS AND NUMERICAL RESULTS

A. Experimental realization

The proposed setup described here may be realized with state-of-the-art experimental techniques. First, the Markovian regime, valid for sufficiently large bias eV, is realized if the Fermi functions of the leads are smooth on a scale set by the natural widths of the levels and residual fluctuations due to the dynamically compensated Overhauser field. Since for typical materials[8] the hyperfine coupling constant is $A_{\mathrm{HF}} = 1$–$100\,\mu$eV and tunneling rates are typically[9] of the order of $\sim 10\,\mu$eV, this does not put a severe restriction on the bias voltage which is routinely[18,19] in the range of hundreds of μV or mV. Second, in order to tune the system into the spin-blockade regime, a sufficiently large external magnetic field has to be applied. More precisely, the corresponding Zeeman splitting ω_0 energetically separates the upper and lower manifolds in such a way that the Fermi function of the right lead drops from one at the lower manifold to zero at the upper manifold. Finite temperature T smears out the Fermi function around the chemical potential by approximately $\sim k_BT$. Accordingly, with cryostatic temperatures of $k_BT \sim 10\,\mu$eV being routinely realized in the laboratory,[10] this condition can be met by applying an external magnetic field of $\sim$5–10 T, which is equivalent to $\omega_0 \approx 100$–$200\,\mu$eV in GaAs.[8,50] The charging energy U, typically $\sim$1–4 meV,[9,19] sets the largest energy scale in the problem justifying the Coulomb-blockade regime with negligible double occupancy of the QD provided that the chemical potential of the left lead is well below the doubly occupied level. Last, we note that similar setups to the one proposed here have previously been realized experimentally by, for example, Hanson *et al.*[26,50]

Proceeding from these considerations, we now show by numerical simulation that an SR peaking of several orders of magnitude can be observed for experimentally relevant parameters in the leakage current through a quantum dot in the spin-blockade regime. We first consider the idealized case of homogeneous coupling for which an exact numerical treatment is feasible even for a larger number of coupled nuclei. Then, we continue with the more realistic case of inhomogeneous coupling for which an approximative scheme is applied. Here, we also study scenarios in which the nuclear spins are not fully polarized initially. Moreover, we discuss intrinsic nuclear dephasing effects and undesired cotunneling processes which have been omitted in our simulations. In particular, we show that the inhomogeneous nature of the HF coupling accounts for the strongest dephasing mechanism in our system. We note that this effect is covered in the second set of our simulations. Finally, we self-consistently justify the perturbative treatment of the Overhauser-field fluctuations as well as the HF flip-flop dynamics.

B. Superradiant electron transport

1. Idealized setting

The homogeneous case allows for an exact treatment even for a relatively large number of nuclei as the system evolves within the totally symmetric low-dimensional subspace $\{|J,m\rangle, m = -J,\ldots,J\}$. Starting from a fully polarized state, a strong intensity enhancement is observed; typical results obtained from numerical simulations of Eq. (30) are depicted in Fig. 5 for $N = 60$ and $N = 100$ nuclear spins. The corresponding relative peak heights display a linear dependence with N (cf. Fig. 6), which we identify as the characteristic feature of SR. Here, we have used the numerical

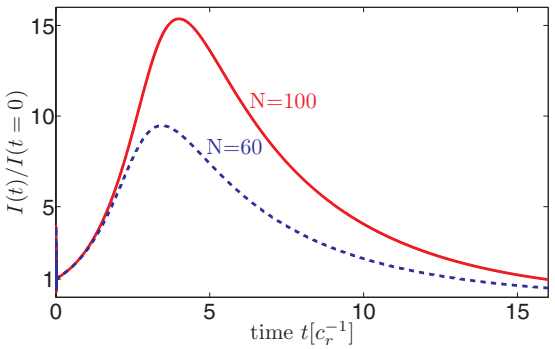

FIG. 5. (Color online) Typical time evolution of the normalized current for homogeneous coupling under dynamical compensation of the Overhauser field and a relative coupling strength of $\epsilon = 0.5$, shown here for $N = 60$ and $N = 100$ nuclear spins. The characteristic feature of SR, a pronounced peak in the leakage current proportional to N, is clearly observed.

parameters $A_{\rm HF} = 1$, $\omega_0 = 1$ and $\alpha = \beta_\uparrow^{(L)} = \beta_\downarrow^{(L)} = \beta_\downarrow^{(R)} = 0.1$ in units of $\sim 100\,\mu$eV, corresponding to a relative coupling strength $\epsilon = 0.5$.

Before we proceed, some further remarks on the dynamic compensation of the Overhauser field seem appropriate: We have merely introduced it in our analysis in order to provide a clear criterion for the presence of purely collective effects, given by $I_{\rm coop}/I_{\rm ind} > 1$. In other words, dynamic compensation of the Overhauser field is not a necessary requirement for the observation of collective effects, but it is rather an adequate tool to display them clearly. From an experimental point of view, the dynamic compensation of the Overhauser field might be challenging as it requires accurate knowledge about the evolution of the nuclear spins. Therefore, we also present results for the case in which the external magnetic field is constant and no compensation is applied. Here, we can distinguish two cases: Depending on the sign of the HF coupling constant $A_{\rm HF}$, the time dependence of the effective

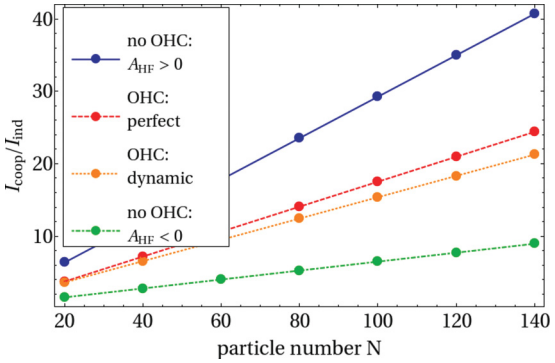

FIG. 6. (Color online) Ratio of the maximum current to the initial current $I_{\rm coop}/I_{\rm ind}$ as a function of the number of nuclear spins N for homogeneous coupling and a relative coupling strength of $\epsilon = 0.5$: Results for perfect compensation (dashed line) are compared to the case of dynamic compensation (dotted line) of the Overhauser field (OHC). Simulations without compensation of the Overhauser field set bounds for the enhancement of the leakage current, depending on the sign of the HF coupling constant $A_{\rm HF}$; solid and dash-dotted line for $A_{\rm HF} > 0$ and $A_{\rm HF} < 0$, respectively.

Zeeman-splitting ω can either give rise to an additional enhancement of the leakage current ($A_{\rm HF} > 0$) or it can counteract the collective effects ($A_{\rm HF} < 0$). As shown in Fig. 6, this sets lower and upper bounds for the observed enhancement of the leakage current.

In Fig. 6 we also compare the results obtained for dynamic compensation of the Overhauser field to the idealized case of perfect compensation in which the effect of the Overhauser term is set to zero, that is, $H_{\rm OH} = g A^z S^z = 0$. Both approaches display the same features justifying our approximation of neglecting residual (de)tuning effects of the dynamically compensated Overhauser field with respect to the external Zeeman splitting ω_0. This is also discussed in greater detail below.

2. *Beyond the idealized setting*

Inhomogeneous HF coupling. In principle, the inhomogeneous HF coupling could prevent the phasing necessary for SR. However, as shown below, SR is still present in realistically inhomogeneous systems. In contrast to the idealized case of homogeneous coupling, the dynamics cannot be restricted to a low-dimensional subspace so that an exact numerical treatment is not feasible due to the large number of nuclei. We therefore use an approximate approach which has previously been shown to capture the effect of nuclear spin coherences while allowing for a numerical treatment of hundreds of spins.[22,27] For simplicity, we restrict ourselves to the local moment regime in which the current can be obtained directly from the electron inversion $I(t) \propto \langle S^+ S^- \rangle_t$. By Eq. (35), this expectation value is related to a hierarchy of correlation terms involving both the electron and the nuclear spins. Based on a Wick type factorization scheme, higher-order expressions are factorized in terms of the covariance matrix $\gamma_{ij}^+ = \langle \sigma_i^+ \sigma_j^- \rangle$ and the "mediated covariance matrix" $\gamma_{ij}^- = \langle \sigma_i^+ S^z \sigma_j^- \rangle$. For further details, see Refs. 22 and 27.

The coupling constants g_j have been obtained from the assumption of a two-dimensional Gaussian spatial electron wave function of width $\sqrt{N}/2$. Specifically, we present results for two sets of numerical parameters, corresponding to a relative coupling strength of $\epsilon = 0.5$, where $A_{\rm HF} = 1, \omega_0 = 1$, $\gamma = 0.1$, and $\Gamma = 0.08$, and $\epsilon = 0.55$ with $A_{\rm HF} = 1, \omega_0 = 0.9$, $\gamma = 0.1$, and $\Gamma = 0.067$.

As shown in Figs. 7 and 8, the results obtained with these methods demonstrate clear SR signatures. In comparison to the ideal case of homogeneous coupling, the relative height is reduced, but for a *fully polarized* initial state we still find a linear enhancement $I_{\rm coop}/I_{\rm ind} \approx 0.043N$ ($\epsilon = 0.5$); therefore, as long as this linear dependence is valid, for typically $N \approx 10^5$–10^6 a strong intensity enhancement of several orders of magnitude is predicted ($\sim 10^3$–10^4).

Imperfect initial polarization. If the initial state is not fully polarized, SR effects are reduced: However, when starting from a mixture of symmetric Dicke states $|J, J\rangle$ with polarization $p = 80(60)\%$, we find that the linear N dependence is still present: $I_{\rm coop}/I_{\rm ind} \approx 0.0075(0.0025)N$ for $\epsilon = 0.5$; that is, the scaling is about a factor of $\sim 5(15)$ weaker than for full polarization.[51] Still, provided the linear scaling holds up to an experimentally realistic number of nuclei $N \approx 10^5$–10^6, this amounts to a relative enhancement of the

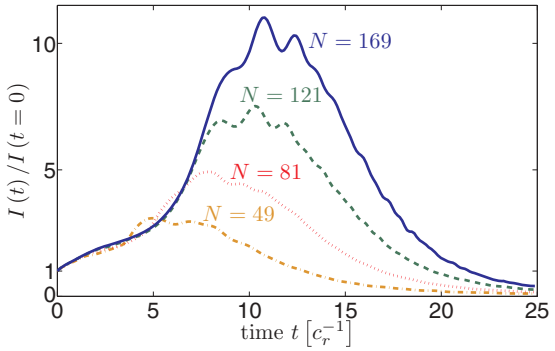

FIG. 7. (Color online) Typical time evolution of the normalized current for inhomogeneous coupling, shown here for up to $N = 13^2$ nuclear spins and a relative coupling strength $\epsilon = 0.55$. Compared to the idealized case of homogeneous coupling, the SR effects are reduced, but still clearly present. A Gaussian spatial electron wave function has been assumed and the Overhauser field is compensated dynamically.

order of $I_{\text{coop}}/I_{\text{ind}} \sim 10^2$–$10^3$. To clearly resolve this peak experimentally, any spurious current should not be larger than the initial HF-mediated leakage current. As we argue below, this condition can be fulfilled in our setup, since the main spurious mechanism, cotunneling, is strongly suppressed.

Nuclear Zeeman term and species inhomogeneity. In our simulations we have disregarded the nuclear Zeeman energies. For a single nuclear species, this term plays no role in the SR dynamics. However, in typical QDs several nuclear species with different g factors are present ("species inhomogeneity"). In principle, these are large enough to cause additional dephasing between the nuclear spins, similar to the inhomogeneous Knight field.[22] However, this dephasing mechanism only applies to nuclei which belong to different species.[22] This leads to few (in GaAs three) mutually decohered subsystems, each of which is described by our theory.

Nuclear interactions. Moreover, we have neglected the dipolar and quadrupolar interactions among the nuclear spins. First, the nuclear dipole-dipole interaction can cause diffusion and dephasing processes. Diffusion processes that can change A^z are strongly detuned by the Knight field and therefore are of minor importance, as corroborated by experimentally measured spin diffusion rates.[52,53] Resonant processes such as $\propto I_i^z I_j^z$ can lead to dephasing similar to the inhomogeneous Knight shift. This competes with the phasing necessary for the observation of SR as expressed by the first term in Eq. (3). The SR process is the weakest at the very beginning of the evolution where we estimate its strength as $c_r^{\min} \approx 10\,\mu\text{eV}/N$. An upper bound for the dipole-dipole interaction in GaAs has been given in Ref. 28 as $\sim 10^{-5}\,\mu$eV, in agreement with values given in Refs. 32 and 41. Therefore, the nuclear dipole-dipole interaction can safely be neglected for $N \lesssim 10^5$. In particular, its dephasing effect should be further reduced for highly polarized ensembles.

Second, the nuclear quadrupolar interactions can have two origins: strain (largely absent in electrically defined QDs) and electric field gradients originating from the electron. These have been estimated for typical electrically defined QDs in Ref. 41 to lead to an additional nuclear level splitting on the order of $\sim 10^{-5}\,\mu$eV. Moreover, they are absent for nuclear spin $I = 1/2$ (e.g., CdSe QDs). To summarize, the additional dephasing mechanisms induced by nuclear interactions are much smaller than the terms arising from the inhomogeneous Knight field.[32] As argued above and confirmed by our simulations, the latter does not prevent the observation of SR behavior due to the presence of the MPM-term in Eq. (3).

3. *Quantitative aspects*

Initially, the HF-mediated SR dynamics is rather slow, with its characteristic time scale set by c_r^{-1}; for experimentally realistic parameters—in what follows we use the parameter set ($\epsilon = 0.5, \alpha \approx 10\,\mu$eV, $N \approx 10^5$) for numerical estimates—this corresponds to $c_r^{-1} \approx 10\,\mu$s. Based on fits as shown in Fig. 9, we then estimate for the SR process duration $\langle t_D \rangle \approx 50 c_r^{-1} \approx 500\,\mu$s, which is still smaller than recently reported[54] nuclear decoherence times of $\sim$1 ms. Therefore, it should be possible to observe the characteristic enhancement of the leakage current before the nuclear spins decohere.

Leakage current. Accordingly, in the initial phasing stage, the HF-mediated lifting of the spin blockade is rather weak, resulting in a low leakage current, approximatively given by $I(t = 0)/(e\hbar^{-1}) \approx \epsilon^2 \alpha / N$. Therefore, the initial current due to HF processes is inversely proportional to the number of nuclear

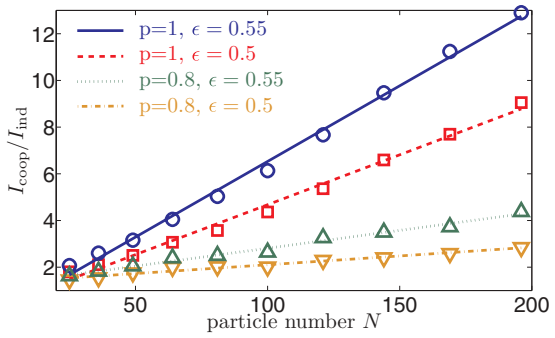

FIG. 8. (Color online) Ratio of the maximum current to the initial current $I_{\text{coop}}/I_{\text{ind}}$ as a function of the number of nuclear spins N for relative coupling strengths $\epsilon = 0.5$ and $\epsilon = 0.55$: Results for inhomogeneous coupling. The linear dependence is still present when starting from a nuclear state with finite polarization $p = 0.8$.

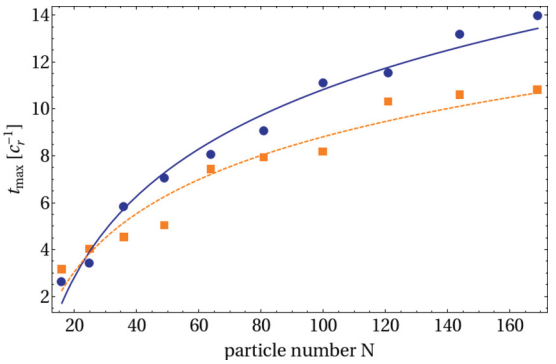

FIG. 9. (Color online) Total time until the observation of the characteristic SR peaking $t_{\max}$ for $\epsilon = 0.5$ (blue dots) and $\epsilon = 0.55$ (orange squares). Based on Eq. (44), logarithmic fits are obtained from which we estimate $t_{\max}$ for experimentally realistic number of nuclear spins $N \approx 10^5$.

spins N. However, as correlations among the nuclei build up, the HF-mediated lifting becomes more efficient, culminating in a maximum current of $I_{\max}/(e\hbar^{-1}) \approx \epsilon^2\alpha$, independent of N. For realistic experimental values—also taking into account the effects of inhomogeneous HF coupling and finite initial polarization $p \approx 0.6$—we estimate the initial (maximum) leakage current to be of the order of $I(t=0) \approx 6$ fA($I_{\max} \approx 10$ pA). Leakage currents in this range of magnitudes have already been detected in single QD spin-filter experiments,[26] as well as double QD Pauli-blockade experiments;[15,16,18,19] here, leakage currents below 10 and 150 fA, respectively, have been attributed explicitly to other spurious processes.[18,26] These are addressed in greater detail in the following.

Our transport setting is tuned into the sequential tunneling regime and therefore we have disregarded cotunneling processes which are fourth order in H_T. In principle, cotunneling processes could lift the spin blockade and add an extra contribution to the leakage current that is independent of the HF dynamics. However, note that cotunneling current scales as $I_{\rm ct} \propto \alpha^2$, whereas sequential tunneling current $I \propto \alpha$; accordingly, cotunneling current can always be suppressed by making the tunnel barriers less transparent.[26] Moreover, inelastic cotunneling processes exciting the QD spin can be ruled out for eV, $k_BT < \omega_0$ due to energy conservation.[25] The effectiveness of a single quantum dot to act as an electrically tunable spin filter has also been demonstrated experimentally:[26] The spin-filter efficiency was measured to be nearly 100%, with $I_{\rm ct}$ being smaller than the noise floor $\sim$10 fA. Its actual value has been calculated as $\sim 10^{-4}$ fA, from which we roughly estimate $I_{\rm ct} \sim 10^{-2}$ fA in our setting. This is smaller than the initial HF-mediated current $I(t=0)$ and considerably smaller than $I_{\max}$, even for an initially not fully polarized nuclear spin ensemble. Still, if one is to explore the regime where cotunneling cannot be neglected, phenomenological dissipative terms—effectively describing the corresponding spin-flip and pure dephasing mechanisms for inelastic and elastic processes, respectively—should be added to Eq. (30).

4. Self-consistency

In our simulations we have self-consistently verified that the fluctuations of the Overhauser field, defined via

$$\Delta_{\rm OH}(t) = g\sqrt{\langle A_z^2\rangle_t - \langle A_z\rangle_t^2}, \tag{48}$$

are indeed small compared to the external Zeeman splitting ω_0 throughout the entire evolution. This ensures the validity of our perturbative approach and the realization of the spin-blockade regime. From atomic SR it is known that in the limit of homogeneous coupling large fluctuations can build up, since in the middle of the emission process the density matrix becomes a broad distribution over the Dicke states.[24] Accordingly, in the idealized, exactly solvable case of homogeneous coupling we numerically find rather large fluctuations of the Overhauser field; as demonstrated in Fig. 10, this holds independently of N. In particular, for a relative coupling strength $\epsilon = 0.5$ the fluctuations culminate in $\max[\Delta_{\rm OH}]/\omega_0 \approx 0.35$. However, in the case of inhomogeneneous HF coupling the Overhauser field fluctuations are found to be smaller as the buildup of these fluctuations is hindered by the Knight term causing dephasing among the nuclear spins. As another limiting case, we also estimate the fluctuations for completely independent homogeneously coupled nuclear spins via the binominal distribution as $\max[\Delta_{\rm OH}] \sim 0.5A_{\rm HF}/\sqrt{N}$ (Ref. 55).

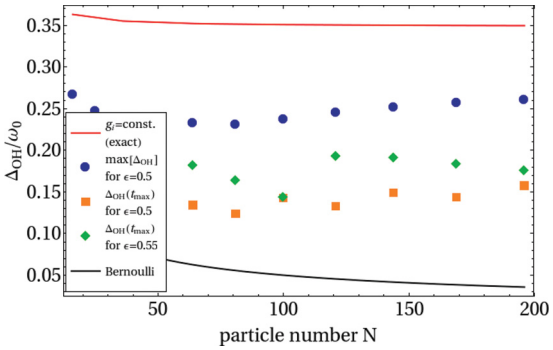

FIG. 10. (Color online) Fluctuations of the Overhauser field relative to the external Zeeman splitting ω_0. In the limit of homogeneous HF coupling, strong fluctuations build up towards the middle of the emission process (red line, $\epsilon = 0.5$). For inhomogeneous coupling this buildup of fluctuations is hindered by the dephasing between the nuclear spins, resulting in considerably smaller fluctuations: The value of the Overhauser fluctuations is shown at the time of the SR peak $t_{\max}$ for $\epsilon = 0.5$ (orange squares) and $\epsilon = 0.55$ (green diamonds). The Overhauser fluctuations reach a maximum value later than $t_{\max}$; see blue dots for $\epsilon = 0.5$. For independent homogeneously coupled nuclear spins, one can estimate the fluctuations via the binominal distribution (black line).

Moreover, we have also ensured self-consistently the validity of the perturbative treatment of the flip-flop dynamics; that is, throughout the entire evolution, even for maximum operative matrix elements $\langle A^+A^-\rangle_t$, the strength of the flip-flop dynamics $\|H_{\rm ff}\|$ was still at least five times smaller than ω_0.

VII. CONCLUSION AND OUTLOOK

In summary, we have developed a master equation based theoretical framework for nuclear-spin-assisted transport through a QD. Due to the collective nature of the HF interaction, it incorporates intriguing many-body effects as well as feedback mechanisms between the electron spin and nuclear spin dynamics. As a prominent application, we have shown that the current through a single electrically defined QD in the spin-blockade regime naturally exhibits superradiant behavior. This effect stems from the collective hyperfine interaction between the QD electron and the nuclear spin ensemble in the QD. Its most striking feature is a lifting of the spin blockade and a pronounced peak in the leakage current. The experimental observation of this effect would provide clear evidence of coherent HF dynamics of nuclear spin ensembles in QDs.

Finally, we highlight possible directions of research going beyond our present work: Apart from superradiant electron transport, the setup proposed here is inherently well suited for other experimental applications like dynamic polarization of nuclear spins (DNPs): In analogy to optical pumping, Eq. (3) describes *electronic* pumping of the nuclear spins. Its steady states are eigenstates of A^z, which lie in the

kernel of the collective jump operator A^-. In particular, for a completely inhomogeneous system the only steady state is the fully polarized one, the ideal initial state required for the observation of SR effects. When starting from a completely unpolarized nuclear state, the unidirectionality of Eq. (3)—electrons with one spin orientation exchange excitations with the nuclear spins, while electrons of opposite spin primarily do not—implies that the rather warm electronic reservoir can still extract entropy out of the nuclear system. More generally, the transport setting studied here possibly opens up the route towards the (feedback-based) electronic preparation of particular nuclear states in single QDs. This is in line with similar ideas previously developed in double QD settings (see, e.g., Refs. 12, 15, 18, 20, and 54).

In this work we have specialized on a single QD. However, our theory could be extended to a double QD (DQD) setting which is likely to offer even more possibilities. DQDs are routinely operated in the Pauli-blockade regime where despite the presence of an applied source-drain voltage the current through the device is blocked whenever the electron tunneling into the DQD has the same spin orientation as the one already present. The DQD parameters and the external magnetic field can be tuned such that the role of the states $|\sigma\rangle, \sigma = \downarrow, \uparrow$, in our model is played by a pair of singlet and triplet states, while all other states are off-resonant. Then, along the lines of our study, nonlinearities appear due to dependencies between the electronic and nuclear subsystems and collective effects enter via the HF-mediated lifting of the spin blockade.

While we have focused on the Markovian regime and the precise conditions for its validity, Eq. (15) offers a starting point for studies of non-Markovian effects in the proposed transport setting. All terms appearing in the memory kernel of Eq. (15) are quadratic in the fermionic creation and annihilation operators allowing for an efficient numerical simulation, without having to explicitly invoke the flatness of the spectral density of the leads. This should then shed light on possibly abrupt changes in the QD transport properties due to feedback mechanism between the nuclear spin ensemble and the electron spin.

Last, our work also opens the door towards studies of dissipative phase transitions in the transport setting: When combined with driving, the SR dynamics can lead to a variety of strong-correlation effects, nonequilibrium, and dissipative phase transitions,[1,56–58] which could now be studied in a mesoscopic solid-state system, complementing other approaches to dissipative phase transitions in QDs.[59–62]

ACKNOWLEDGMENTS

We thank O. Viyuela for fruitful discussions. We acknowledge support by the DFG within SFB 631 and the Cluster of Excellence NIM.

APPENDIX A: MICROSCOPIC DERIVATION OF THE MASTER EQUATION

In this appendix we provide some details regarding the derivation of the master equations as stated in Eqs. (2) and (30). It comprises the effect of the HF dynamics in the memory kernel of Eq. (13) and the subsequent approximation of independent rates of variation.

In the following, we show that it is self-consistent to neglect the effect of the HF dynamics $\mathcal{L}_1(t)$ in the memory kernel of Eq. (13) provided that the bath correlation time τ_c is short compared to the Rabi flips produced by the HF dynamics. This needs to be addressed as cooperative effects potentially drive the system from a weakly coupled into a strongly coupled regime. First, we reiterate the Schwinger-Dyson identity in Eq. (14) as an infinite sum over time-ordered nested commutators

$$e^{-i(\mathcal{L}_0+\mathcal{L}_1)\tau} = e^{-i\mathcal{L}_0\tau}\sum_{n=0}^{\infty}(-i)^n\int_0^\tau d\tau_1\int_0^{\tau_1}d\tau_2\ldots \times\int_0^{\tau_{n-1}}d\tau_n\,\tilde{\mathcal{L}}_1(\tau_1)\tilde{\mathcal{L}}_1(\tau_2)\ldots\tilde{\mathcal{L}}_1(\tau_n), \quad \text{(A1)}$$

where for any operator X

$$\tilde{\mathcal{L}}_1(\tau)X = e^{i\mathcal{L}_0\tau}\mathcal{L}_1 e^{-i\mathcal{L}_0\tau}X = [e^{iH_0\tau}H_1e^{-iH_0\tau},X] = [\tilde{H}_1(\tau),X]. \quad \text{(A2)}$$

More explicitly, up to second order Eq. (A1) is equivalent to

$$e^{-i(\mathcal{L}_0+\mathcal{L}_1)\tau}X = e^{-i\mathcal{L}_0\tau}X - ie^{-i\mathcal{L}_0\tau}\int_0^\tau d\tau_1[\tilde{H}_1(\tau_1),X] - e^{-i\mathcal{L}_0\tau}\int_0^\tau d\tau_1\int_0^{\tau_1}d\tau_2[\tilde{H}_1(\tau_1),[\tilde{H}_1(\tau_2),X]]+\cdots. \quad \text{(A3)}$$

Note that the time dependence of $\tilde{H}_1(\tau)$ is simply given by

$$\tilde{H}_1(\tau) = e^{i\omega\tau}H_+ + e^{-i\omega\tau}H_- + H_{\Delta\mathrm{OH}}, \quad H_\pm = \frac{g}{2}S^\pm A^\mp, \quad \text{(A4)}$$

where the effective Zeeman splitting $\omega = \omega_0 + g\langle A^z\rangle_t$ is time dependent. Accordingly, we define $\tilde{\mathcal{L}}_1(\tau) = \tilde{\mathcal{L}}_+(\tau) + \tilde{\mathcal{L}}_-(\tau) + \tilde{\mathcal{L}}_{\Delta\mathrm{OH}}(\tau) = e^{i\omega\tau}\mathcal{L}_+ + e^{-i\omega\tau}\mathcal{L}_- + \mathcal{L}_{\Delta\mathrm{OH}}$, where $\mathcal{L}_x\cdot = [H_x,\cdot]$ for $x = \pm,\Delta\mathrm{OH}$. In the next steps, we explicitly evaluate the first two contributions to the memory kernel that go beyond $n = 0$ and then generalize our findings to any order n of the Schwinger-Dyson series.

1. First-order correction

The first-order contribution $n = 1$ in Eq. (13) is given by

$$\Xi^{(1)} = i\int_0^t d\tau\int_0^\tau d\tau_1\,\mathrm{Tr}_B(\mathcal{L}_T e^{-i\mathcal{L}_0\tau}[\tilde{H}_1(\tau_1),X]). \quad \text{(A5)}$$

Performing the integration in τ_1 leads to

$$\Xi^{(1)} = \int_0^t d\tau\left\{\frac{g}{2\omega}(1-e^{-i\omega\tau})\mathrm{Tr}_B(\mathcal{L}_T[S^+A^-,\tilde{X}_\tau]) + \frac{g}{2\omega}(e^{i\omega\tau}-1)\mathrm{Tr}_B(\mathcal{L}_T[S^-A^+,\tilde{X}_\tau]) + ig\tau\,\mathrm{Tr}_B(\mathcal{L}_T[(A^z-\langle A^z\rangle_t)S^z,\tilde{X}_\tau])\right\}, \quad \text{(A6)}$$

where, for notational convenience, we introduced the operators $X = \mathcal{L}_T\rho_S(t-\tau)\rho_B^0$ and $\tilde{X}_\tau = e^{-iH_0\tau}[H_T,\rho_S(t-\tau)\rho_B^0]e^{iH_0\tau} \approx [\tilde{H}_T(\tau),\rho_S(t)\rho_B^0]$. In accordance with previous

approximations, we have replaced $e^{-iH_0\tau}\rho_S(t-\tau)e^{iH_0\tau}$ with $\rho_S(t)$ since any additional term besides H_0 would be of higher order in perturbation theory.[35,36] In particular, this disregards dissipative effects: In our case, this approximation is valid self-consistently provided that the tunneling rates are small compared to effective Zeeman splitting ω. The integrand decays on the leads-correlation time scale τ_c, which is typically much faster than the time scale set by the effective Zeeman splitting, $\omega\tau_c \ll 1$. This separation of time scales allows for an expansion in the small parameter $\omega\tau$, for example, $\frac{g}{\omega}(e^{i\omega\tau}-1) \approx ig\tau$. We see that the first-order correction can be neglected if the the bath correlation time τ_c is sufficiently short compared to the time scale of the HF dynamics, that is $g\tau_c \ll 1$. The latter is bounded by the total hyperfine coupling constant A_{HF} (since $||gA^x|| \leqslant A_{\mathrm{HF}}$) so that the requirement for disregarding the first-order term reads $A_{\mathrm{HF}}\tau_c \ll 1$.

2. Second-order correction

The contribution of the second term $n=2$ in the Schwinger-Dyson expansion can be decomposed into

$$\Xi^{(2)} = \Xi^{(2)}_{\mathrm{zz}} + \Xi^{(2)}_{\mathrm{ff}} + \Xi^{(2)}_{\mathrm{fz}}. \tag{A7}$$

The first term $\Xi^{(2)}_{\mathrm{zz}}$ contains contributions from $H_{\Delta\mathrm{OH}}$ only,

$$\begin{aligned}\Xi^{(2)}_{\mathrm{zz}} &= \int_0^t d\tau \int_0^\tau d\tau_1 \int_0^{\tau_1} d\tau_2 \mathsf{Tr}_{\mathsf{B}}(\mathcal{L}_T e^{-i\mathcal{L}_0\tau}[\tilde{H}_{\Delta\mathrm{OH}}(\tau_1), \\ &\quad [\tilde{H}_{\Delta\mathrm{OH}}(\tau_2), X]]) \qquad \text{(A8)}\\ &= -\int_0^t d\tau (g\tau)^2 \mathsf{Tr}_{\mathsf{B}}\Big[\mathcal{L}_T\Big(\delta A^z S^z \tilde{X}_\tau \delta A^z S^z \\ &\quad - \frac{1}{2}\{\delta A^z S^z \delta A^z S^z, \tilde{X}_\tau\}\Big)\Big]. \qquad \text{(A9)}\end{aligned}$$

Similarly, $\Xi^{(2)}_{\mathrm{ff}}$, which comprises contributions from H_{ff} only is found to be

$$\begin{aligned}\Xi^{(2)}_{\mathrm{ff}} &= \frac{g^2}{4\omega^2}\int_0^t d\tau\{(1+i\omega\tau-e^{i\omega\tau}) \\ &\quad \times \mathsf{Tr}_{\mathsf{B}}[\mathcal{L}_T(S^+S^-A^-A^+\tilde{X}_\tau + \tilde{X}_\tau S^-S^+A^+A^-)] \\ &\quad + (1-i\omega\tau-e^{-i\omega\tau})\mathsf{Tr}_{\mathsf{B}}[\mathcal{L}_T(S^-S^+A^+A^-\tilde{X}_\tau \\ &\quad + \tilde{X}_\tau S^+S^-A^-A^+)]\}. \qquad \text{(A10)}\end{aligned}$$

Here, we have used the following simplification: The time-ordered products which include flip-flop terms only can be simplified to two possible sequences in which $\mathcal{L}_+$ is followed by $\mathcal{L}_-$ and vice versa. This holds since

$$\begin{aligned}\mathcal{L}_\pm\mathcal{L}_\pm X &= [H_\pm,[H_\pm,X]] \\ &= H_\pm H_\pm X + X H_\pm H_\pm - 2H_\pm X H_\pm = 0. \qquad \text{(A11)}\end{aligned}$$

Here, the first two terms drop out immediately since the electronic jump operators $S^\pm$ fulfill the relation $S^\pm S^\pm = 0$. In the problem at hand, also the last term gives zero because of particle number superselection rules: In Eq. (13) the time-ordered product of superoperators acts on $X = [H_T, \rho_S(t-\tau)\rho_B^0]$. Thus, for the term $H_\pm X H_\pm$ to be nonzero, coherences in Fock space would be required, which are consistently neglected (compare Ref. 36). This is equivalent to ignoring coherences between the system and the leads. Note that the same argument holds for any combination $H_\mu X H_\nu$ with $\mu,\nu = \pm$.

Similar results can be obtained for $\Xi^{(2)}_{\mathrm{fz}}$ which comprises $H_\pm$ as well as $H_{\Delta\mathrm{OH}}$ in all possible orderings. Again, using that the integrand decays on a time scale τ_c and expanding in the small parameter $\omega\tau$ shows that the second-order contribution scales as $\sim(g\tau_c)^2$. Our findings for the first- and second-order correction suggest that the nth-order correction scales as $\sim(g\tau_c)^n$. This is proven in the following by induction.

3. nth-order correction

The scaling of the nth term in the Dyson series is governed by the quantities of the form

$$\xi^{(n)}_{+-\ldots}(\tau) = g^n \int_0^\tau d\tau_1 \int_0^{\tau_1} d\tau_2 \cdots \int_0^{\tau_{n-1}} d\tau_n e^{i\omega\tau_1} e^{-i\omega\tau_2} \ldots, \tag{A12}$$

where the index suggests the order in which $H_\pm$ (giving an exponential factor) and $H_{\Delta\mathrm{OH}}$ (resulting in a factor of 1) appear. Led by our findings for $n=1,2$, we claim that the expansion of $\xi^{(n)}_{+-\ldots}(\tau)$ for small $\omega\tau$ scales as $\xi^{(n)}_{+-\ldots}(\tau) \sim (g\tau)^n$. Then, the $(n+1)$th terms scale as

$$\begin{aligned}\xi^{(n+1)}_{-(\Delta\mathrm{OH})+-\ldots}(\tau) &= g^{n+1}\int_0^\tau d\tau_1 \int_0^{\tau_1} d\tau_2 \cdots \int_0^{\tau_{n-1}} d\tau_n \\ &\quad \times \int_0^{\tau_n} d\tau_{n+1} \begin{pmatrix} e^{-i\omega\tau_1} \\ 1 \end{pmatrix} e^{+i\omega\tau_2} \cdots \qquad \text{(A13)}\\ &= g\int_0^\tau d\tau_1 \begin{pmatrix} e^{-i\omega\tau_1} \\ 1 \end{pmatrix} \xi^{(n)}_{+-\ldots}(\tau_1) \qquad \text{(A14)}\\ &\sim (g\tau)^{n+1}. \qquad \text{(A15)}\end{aligned}$$

Since we have already verified this result for $n=1,2$, the general result follows by induction. This completes the proof.

APPENDIX B: ADIABATIC ELIMINATION OF THE QD ELECTRON

For a sufficiently small relative coupling strength ϵ the nuclear dynamics are slow compared to the electronic QD dynamics. This allows for an adiabatic elimination of the electronic degrees of freedom yielding an effective master equation for the nuclear spins of the QD.

Our analysis starts out from Eq. (35), which we write as

$$\dot{\rho} = \mathcal{W}_0\rho + \mathcal{W}_1\rho, \tag{B1}$$

where

$$\begin{aligned}\mathcal{W}_0\rho &= -i[\omega_0 S^z,\rho] + \gamma\left[S^-\rho S^+ - \frac{1}{2}\{S^+S^-,\rho\}\right] \\ &\quad + \Gamma\left[S^z\rho S^z - \frac{1}{4}\rho\right], \qquad \text{(B2)}\\ \mathcal{W}_1\rho &= -i[H_{\mathrm{HF}},\rho]. \qquad \text{(B3)}\end{aligned}$$

Note that the superoperator $\mathcal{W}_0$ only acts on the electronic degrees of freedom. It describes an electron in an external magnetic field that experiences a decay as well as a pure dephasing mechanism. In zeroth order of the coupling parameter

ϵ the electronic and nuclear dynamics of the QD are decoupled and SR effects cannot be expected. These are contained in the interaction term $\mathcal{W}_1$.

Formally, the adiabatic elimination of the electronic degrees of freedom can be achieved as follows:[63] To zeroth order in ϵ the eigenvectors of $\mathcal{W}_0$ with zero eigenvector $\lambda_0 = 0$ are

$$\mathcal{W}_0 \mu \otimes \rho_{SS} = 0, \tag{B4}$$

where $\rho_{SS} = |\downarrow\rangle\langle\downarrow|$ is the stationary solution for the electronic dynamics and μ describes some arbitrary state of the nuclear system. The zeroth-order Liouville eigenstates corresponding to $\lambda_0 = 0$ are coupled to the subspaces of "excited" nonzero (complex) eigenvalues $\lambda_k \neq 0$ of $\mathcal{W}_0$ by the action of $\mathcal{W}_1$. Physically, this corresponds to a coupling between electronic and nuclear degrees of freedom. In the limit where the HF dynamics are slow compared to the electronic frequencies, that is, the Zeeman splitting ω_0, the decay rate γ, and the dephasing rate Γ, the coupling between these blocks of eigenvalues and Liouville subspaces of $\mathcal{W}_0$ is weak, justifying a perturbative treatment. This motivates the definition of a projection operator P onto the subspace with zero eigenvalue $\lambda_0 = 0$ of $\mathcal{W}_0$ according to

$$P\rho = \mathrm{Tr}_{\mathrm{el}}[\rho] \otimes \rho_{SS} = \mu \otimes |\downarrow\rangle\langle\downarrow|, \tag{B5}$$

where $\mu = \mathrm{Tr}_{\mathrm{el}}[\rho]$ is a density operator for the nuclear spins, $\mathrm{Tr}_{\mathrm{el}} \ldots$ denotes the trace over the electronic subspace, and, by definition, $\mathcal{W}_0 \rho_{SS} = 0$. The complement of P is $Q = 1 - P$. By projecting the master equation on the P subspace and tracing over the electronic degrees of freedom we obtain an effective master equation for the nuclear spins in second-order perturbation theory,

$$\dot{\mu} = \mathrm{Tr}_{\mathrm{el}}\big[P\mathcal{W}_1 P\rho - P\mathcal{W}_1 Q\mathcal{W}_0^{-1} Q\mathcal{W}_1 P\rho\big]. \tag{B6}$$

Using $\mathrm{Tr}_{\mathrm{el}}[S^z \rho_{SS}] = -1/2$, the first term is readily evaluated and yields the Knight shift seen by the nuclear spins,

$$\mathrm{Tr}_{\mathrm{el}}[P\mathcal{W}_1 P\rho] = +i\frac{g}{2}[A^z,\mu]. \tag{B7}$$

The derivation of the second term is more involved. It can be rewritten as

$$\begin{aligned} &-\mathrm{Tr}_{\mathrm{el}}\big[P\mathcal{W}_1 Q\mathcal{W}_0^{-1} Q\mathcal{W}_1 P\rho\big] \\ &\quad = -\mathrm{Tr}_{\mathrm{el}}\big[P\mathcal{W}_1(1-P)\mathcal{W}_0^{-1}(1-P)\mathcal{W}_1 P\rho\big] \qquad \text{(B8)} \\ &\quad = \int_0^\infty d\tau\, \mathrm{Tr}_{\mathrm{el}}[P\mathcal{W}_1 e^{\mathcal{W}_0\tau}\mathcal{W}_1 P\rho] \\ &\qquad - \int_0^\infty d\tau\, \mathrm{Tr}_{\mathrm{el}}[P\mathcal{W}_1 P\mathcal{W}_1 P\rho]. \qquad \text{(B9)} \end{aligned}$$

Here, we used the Laplace transform $-\mathcal{W}_0^{-1} = \int_0^\infty d\tau\, e^{\mathcal{W}_0\tau}$ and the property $e^{\mathcal{W}_0\tau}P = Pe^{\mathcal{W}_0\tau} = P$.

Let us first focus on the first term in Eq. (B9). It contains terms of the form

$$\begin{aligned} &\mathrm{Tr}_{\mathrm{el}}[P[A^+S^-, e^{\mathcal{W}_0\tau}[A^-S^+, \mu\otimes\rho_{SS}]]] \\ &\quad = \mathrm{Tr}_{\mathrm{el}}[S^- e^{\mathcal{W}_0\tau}(S^+\rho_{SS})]A^+A^-\mu \qquad \text{(B10)} \\ &\qquad - \mathrm{Tr}_{\mathrm{el}}[S^- e^{\mathcal{W}_0\tau}(S^+\rho_{SS})]A^-\mu A^+ \qquad \text{(B11)} \\ &\qquad + \mathrm{Tr}_{\mathrm{el}}[S^- e^{\mathcal{W}_0\tau}(\rho_{SS}S^+)]\mu A^-A^+ \qquad \text{(B12)} \\ &\qquad - \mathrm{Tr}_{\mathrm{el}}[S^- e^{\mathcal{W}_0\tau}(\rho_{SS}S^+)]A^+\mu A^-. \qquad \text{(B13)} \end{aligned}$$

This can be simplified using the following relations: Since $\rho_{SS} = |\downarrow\rangle\langle\downarrow|$, we have $S^-\rho_{SS} = 0$ and $\rho_{SS}S^+ = 0$. Moreover, $|\uparrow\rangle\langle\downarrow|$ and $|\downarrow\rangle\langle\uparrow|$ are eigenvectors of $\mathcal{W}_0$ with eigenvalues $-(i\omega_0 + \alpha/2)$ and $+(i\omega_0 - \alpha/2)$, where $\alpha = \gamma + \Gamma$, yielding

$$e^{\mathcal{W}_0\tau}(S^+\rho_{SS}) = e^{-(i\omega_0+\alpha/2)\tau}|\uparrow\rangle\langle\downarrow|, \tag{B14}$$

$$e^{\mathcal{W}_0\tau}(\rho_{SS}S^-) = e^{+(i\omega_0-\alpha/2)\tau}|\downarrow\rangle\langle\uparrow|. \tag{B15}$$

This leads to

$$\begin{aligned} &\mathrm{Tr}_{\mathrm{el}}[P[A^+S^-, e^{\mathcal{W}_0\tau}[A^-S^+, \mu\otimes\rho_{SS}]]] \\ &\quad = e^{-(i\omega_0+\alpha/2)\tau}(A^+A^-\mu - A^-\mu A^+). \end{aligned} \tag{B16}$$

Similarly, one finds

$$\begin{aligned} &\mathrm{Tr}_{\mathrm{el}}[P[A^-S^+, e^{\mathcal{W}_0\tau}[A^+S^-, \mu\otimes\rho_{SS}]]] \\ &\quad = e^{+(i\omega_0-\alpha/2)\tau}(\mu A^+A^- - A^-\mu A^+). \end{aligned} \tag{B17}$$

Analogously, one can show that terms containing two flip or two flop terms give zero. The same holds for mixed terms that comprise one flip-flop and one Overhauser term with $\sim A^zS^z$. The term consisting of two Overhauser contributions gives

$$\begin{aligned} &\mathrm{Tr}_{\mathrm{el}}[P[A^zS^z, e^{\mathcal{W}_0\tau}[A^zS^z, \mu\otimes\rho_{SS}]]] \\ &\quad = -\tfrac{1}{4}[2A^z\mu A^z - [A^zA^z, \mu]]. \end{aligned} \tag{B18}$$

However, this term exactly cancels with the second term from Eq. (B9). Thus, we are left with the contributions coming from Eqs. (B16) and (B17). Restoring the prefactors of $-ig/2$, we obtain

$$\begin{aligned} &\mathrm{Tr}_{\mathrm{el}}\big[P\mathcal{W}_1 Q\big(-\mathcal{W}_0^{-1}\big)Q\mathcal{W}_1 P\rho\big] \\ &\quad = \frac{g^2}{4}\int_0^\infty d\tau[e^{-(i\omega_0+\alpha/2)\tau}(A^-\mu A^+ - A^+A^-\mu) \\ &\qquad + e^{+(i\omega_0-\alpha/2)\tau}(A^-\mu A^+ - \mu A^+A^-)]. \end{aligned} \tag{B19}$$

Performing the integration and separating real from imaginary terms yields

$$\begin{aligned} &\mathrm{Tr}_{\mathrm{el}}\big[P\mathcal{W}_1 Q\big(-\mathcal{W}_0^{-1}\big)Q\mathcal{W}_1 P\rho\big] \\ &\quad = c_r\left[A^-\mu A^+ - \frac{1}{2}\{A^+A^-, \mu\}\right] + ic_i[A^+A^-, \mu], \end{aligned} \tag{B20}$$

where $c_r = g^2/(4\omega_0^2 + \alpha^2)\alpha$ and $c_i = g^2/(4\omega_0^2 + \alpha^2)\omega_0$. Combining Eq. (B7) with Eq. (B20) directly gives the effective master equation for the nuclear spins given in Eq. (3) in the main text.

[1] T. Brandes, Phys. Rep. **408**, 315 (2004).

[2] D. D. Awschalom, N. Samarth, and D. Loss, *Semiconductor Spintronics and Quantum Computation* (Springer-Verlag, Berlin, 2002).

[3] D. Y. Sharvin and Y. V. Sharvin, JETP Lett. **34**, 272 (1981).

[4] B. J. van Wees, H. van Houten, C. W. J. Beenakker, J. G. Williamson, L. P. Kouwenhoven, D. van der Marel, and C. T. Foxon, Phys. Rev. Lett. **60**, 848 (1988).

[5] D. Wharam, T. J. Thornton, R. Newbury, M. Pepper, H. Ahmed, J. E. F. Frost, D. G. Husko, D. C. Peacock, D. A. Ritchie, and G. A. C. Jones, J. Phys. C **21**, 209 (1988).

[6] Y. V. Nazarov and Y. M. Blanter, *Quantum Transport* (Cambridge University Press, Cambridge, 2009).

[7] S. Datta, *Electronic Transport in Mesoscopic Systems* (Cambridge University Press, Cambridge, 1997).

[8] R. Hanson, L. P. Kouwenhoven, J. R. Petta, S. Tarucha, and L. M. Vandersypen, Rev. Mod. Phys. **79**, 1217 (2007).

[9] W. G. van der Wiel, S. De Franceschi, J. M. Elzerman, T. Fujisawa, S. Tarucha, and L. P. Kouwenhoven, Rev. Mod. Phys. **75**, 1 (2002).

[10] A. C. Johnson, J. R. Petta, J. M. Taylor, A. Yacoby, M. D. Lukin, C. M. Marcus, M. P. Hanson, and A. C. Gossard, Nature (London) **435**, 925 (2005).

[11] O. N. Jouravlev and Y. V. Nazarov, Phys. Rev. Lett. **96**, 176804 (2006).

[12] J. Baugh, Y. Kitamura, K. Ono, and S. Tarucha, Phys. Rev. Lett. **99**, 096804 (2007).

[13] J. R. Petta, J. M. Taylor, A. C. Johnson, A. Yacoby, M. D. Lukin, C. M. Marcus, M. P. Hanson, and A. C. Gossard, Phys. Rev. Lett. **100**, 067601 (2008).

[14] J. Iñarrea, G. Platero, and A. H. MacDonald, Phys. Rev. B **76**, 085329 (2007).

[15] F. H. L. Koppens, J. A. Folk, J. M. Elzerman, R. Hanson, L. H. Willems van Beveren, I. T. Vink, H. P. Tranitz, W. Wegschneider, L. P. Kouwenhoven, and L. M. K. Vandersypen, Science **309**, 1346 (2005).

[16] K. Ono and S. Tarucha, Phys. Rev. Lett. **92**, 256803 (2004).

[17] A. Pfund, I. Shorubalko, K. Ensslin, and R. Leturcq, Phys. Rev. Lett. **99**, 036801 (2007).

[18] T. Kobayashi, K. Hitachi, S. Sasaki, and K. Muraki, Phys. Rev. Lett. **107**, 216802 (2011).

[19] K. Ono, D. G. Austing, Y. Tokura, and S. Tarucha, Science **297**, 1313 (2002).

[20] M. S. Rudner and L. S. Levitov, Phys. Rev. Lett. **99**, 036602 (2007).

[21] M. Eto, T. Ashiwa, and M. Murata, J. Phys. Soc. Jpn. **73**, 307 (2004).

[22] H. Christ, J. I. Cirac, and G. Giedke, Phys. Rev. B **75**, 155324 (2007).

[23] R. H. Dicke, Phys. Rev. **93**, 99 (1954).

[24] M. Gross and S. Haroche, Phys. Rep. **93**, 301 (1982).

[25] P. Recher, E. V. Sukhorukov, and Daniel Loss, Phys. Rev. Lett. **85**, 1962 (2000).

[26] R. Hanson, L. M. K. Vandersypen, L. H. Willems van Beveren, J. M. Elzerman, I. T. Vink, and L. P. Kouwenhoven, Phys. Rev. B **70**, 241304(R) (2004).

[27] E. M. Kessler, S. Yelin, M. D. Lukin, J. I. Cirac, and G. Giedke, Phys. Rev. Lett. **104**, 143601 (2010).

[28] J. Schliemann, A. Khaetskii, and Daniel Loss, J. Phys.: Condens. Matter **15**, R1809 (2003).

[29] H. Bruus and K. Flensberg, *Many-Body Quantum Theory in Condensed Matter Physics* (Oxford University Press, New York, 2006).

[30] Y. Yamamoto and A. Imamoglu, *Mesoscopic Quantum Optics* (Wiley, New York, 1999).

[31] S. Welack, M. Esposito, U. Harbola, and S. Mukamel, Phys. Rev. B **77**, 195315 (2008).

[32] J. M. Taylor, J. R. Petta, A. C. Johnson, A. Yacoby, C. M. Marcus, and M. D. Lukin, Phys. Rev. B **76**, 035315 (2007).

[33] C. Cohen-Tannoudji, J. Dupont-Roc, and G. Grynberg, *Atom-Photon Interactions: Basic Processes and Applications* (Wiley, New York, 1992).

[34] C. Timm (private communication).

[35] C. Timm, Phys. Rev. B **77**, 195416 (2008).

[36] U. Harbola, M. Esposito, and S. Mukamel, Phys. Rev. B **74**, 235309 (2006).

[37] H.-A. Engel and D. Loss, Phys. Rev. B **65**, 195321 (2002).

[38] N. Zhao, J.-L. Zhu, R.-B. Liu, and C. P. Sun, New J. Phys. **13**, 013005 (2011).

[39] S. A. Gurvitz and Ya. S. Prager, Phys. Rev. B **53**, 15932 (1996).

[40] S. A. Gurvitz, Phys. Rev. B **57**, 6602 (1998).

[41] H. Bluhm, S. Foletti, I. Neder, M. Rudner, D. Mahalu, V. Umansky, and A. Yacoby, Nat. Phys. **7**, 109 (2010).

[42] G. S. Agrawal, Phys. Rev. A **4**, 1791 (1971).

[43] C. Leonardi and A. Vaglica, Nuovo Cimento Soc. Ital. Fis. B **67**, 256 (1982).

[44] V. V. Temnov and U. Woggon, Phys. Rev. Lett. **95**, 243602 (2005).

[45] D. A. Bagrets and Yu. V. Nazarov, Phys. Rev. B **67**, 085316 (2003).

[46] M. Esposito, U. Harbola, and S. Mukamel, Rev. Mod. Phys. **81**, 1665 (2009).

[47] C. Emary, C. Pöltl, A. Carmele, J. Kabuss, A. Knorr, and T. Brandes, Phys. Rev. B **85**, 165417 (2012).

[48] L. D. Contreras-Pulido and R. Aguado, Phys. Rev. B **81**, 161309(R) (2010).

[49] H. J. Carmichael, *Statistical Methods in Quantum Optics 1* (Springer, Berlin, 1999).

[50] R. Hanson, B. Witkamp, L. M. K. Vandersypen, L. H. Willems van Beveren, J. M. Elzerman, and L. P. Kouwenhoven, Phys. Rev. Lett. **91**, 196802 (2003).

[51] For finite polarization the initial covariance matrix has been determined heuristically from the dark-state condition $\langle A^- A^+ \rangle = 0$ in the homogeneous limit.

[52] D. Paget, Phys. Rev. B **25**, 4444 (1982).

[53] T. Ota, G. Yusa, N. Kumada, S. Miyashita, T. Fujisawa, and Y. Hirayama, Appl. Phys. Lett. **91**, 193101 (2007).

[54] R. Takahashi, K. Kono, S. Tarucha, and K. Ono, Phys. Rev. Lett. **107**, 026602 (2011).

[55] This limit is realized if strong nuclear dephasing processes prevent the coherence buildup of the SR evolution.

[56] H. J. Carmichael, J. Phys. B **13**, 3551 (1980).

[57] S. Morrison and A. S. Parkins, Phys. Rev. A **77**, 043810 (2008).

[58] E. M. Kessler, G. Giedke, A. Imamoglu, S. F. Yelin, M. D. Lukin, and J. I. Cirac, Phys. Rev. A **86**, 012116 (2012).

[59] C.-H. Chung, K. Le Hur, M. Vojta, and P. Wölfle, Phys. Rev. Lett. **102**, 216803 (2009).

[60] L. Borda, G. Zarand, and D. Goldhaber-Gordon, arXiv:cond-mat/0602019.

[61] A. J. Leggett, S. Chakravarty, A. T. Dorsey, M. P. A. Fisher, A. Garg, and W. Zwerger, Rev. Mod. Phys. **59**, 1 (1987).

[62] M. S. Rudner and L. S. Levitov, Phys. Rev. B **82**, 155418 (2010).

[63] J. I. Cirac, R. Blatt, P. Zoller, and W. D. Phillips, Phys. Rev. A **46**, 2668 (1992).